

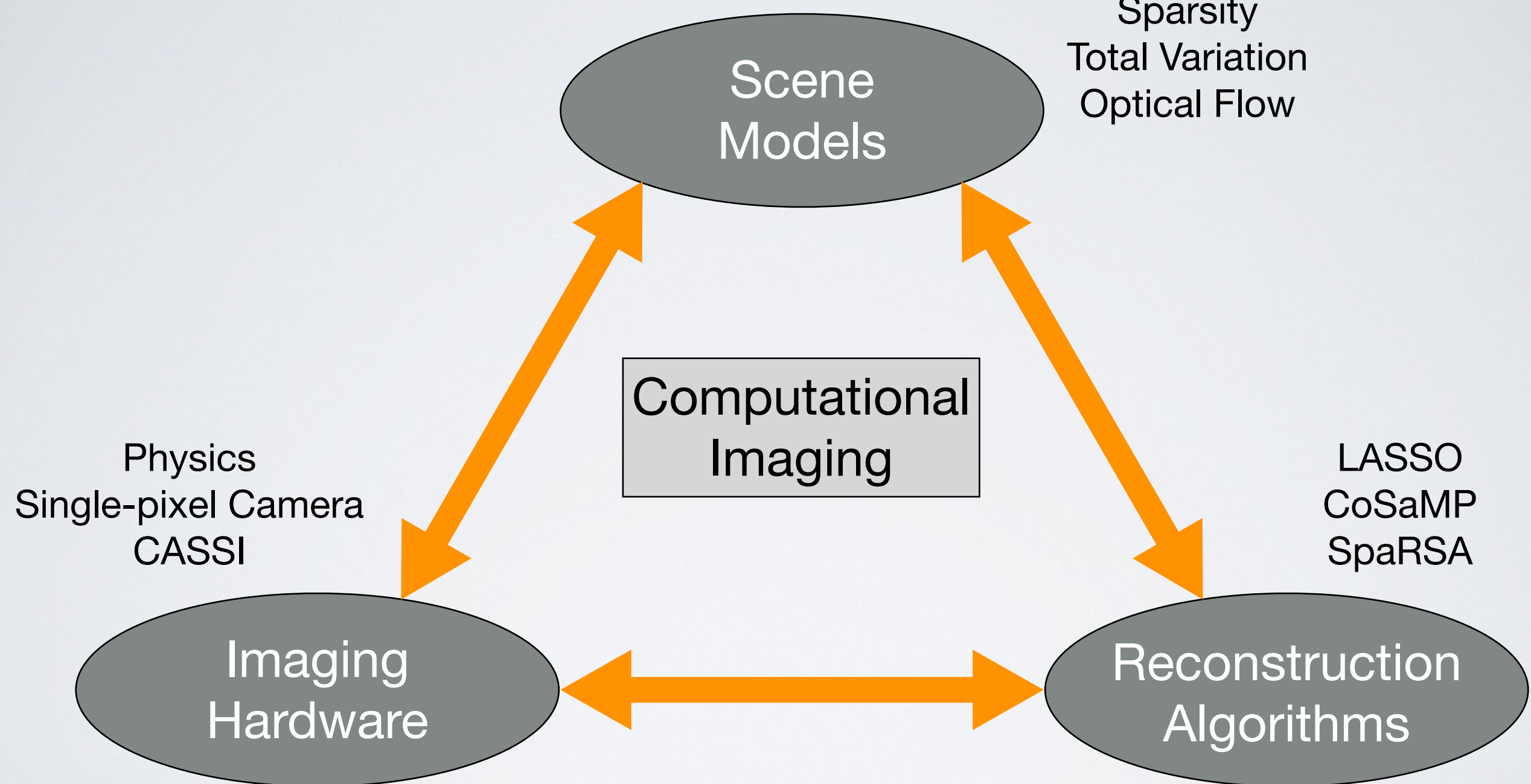
Computational Optical Imaging Systems: Sensing Strategies, Optimization Methods, and Performance Bounds

Zachary T. Harmany
PhD Dissertation Defense
October 23, 2012

Advisor
Rebecca Willett

Committee
Robert Calderbank, Guillermo Sapiro,
Roummel Marcia, Nimmi Ramanujam

Computational Imaging



Challenges for Computational Imaging

- Aren't pixels cheap?
iPhone 5 camera: 8MP for \$18.00¹
- Not when light is scarce
PMT: 1 pixel for \$1,000.00²
- Or out of visible range
SWIR: 100-500X per-pixel cost⁴



SWIR penetrates fog⁵

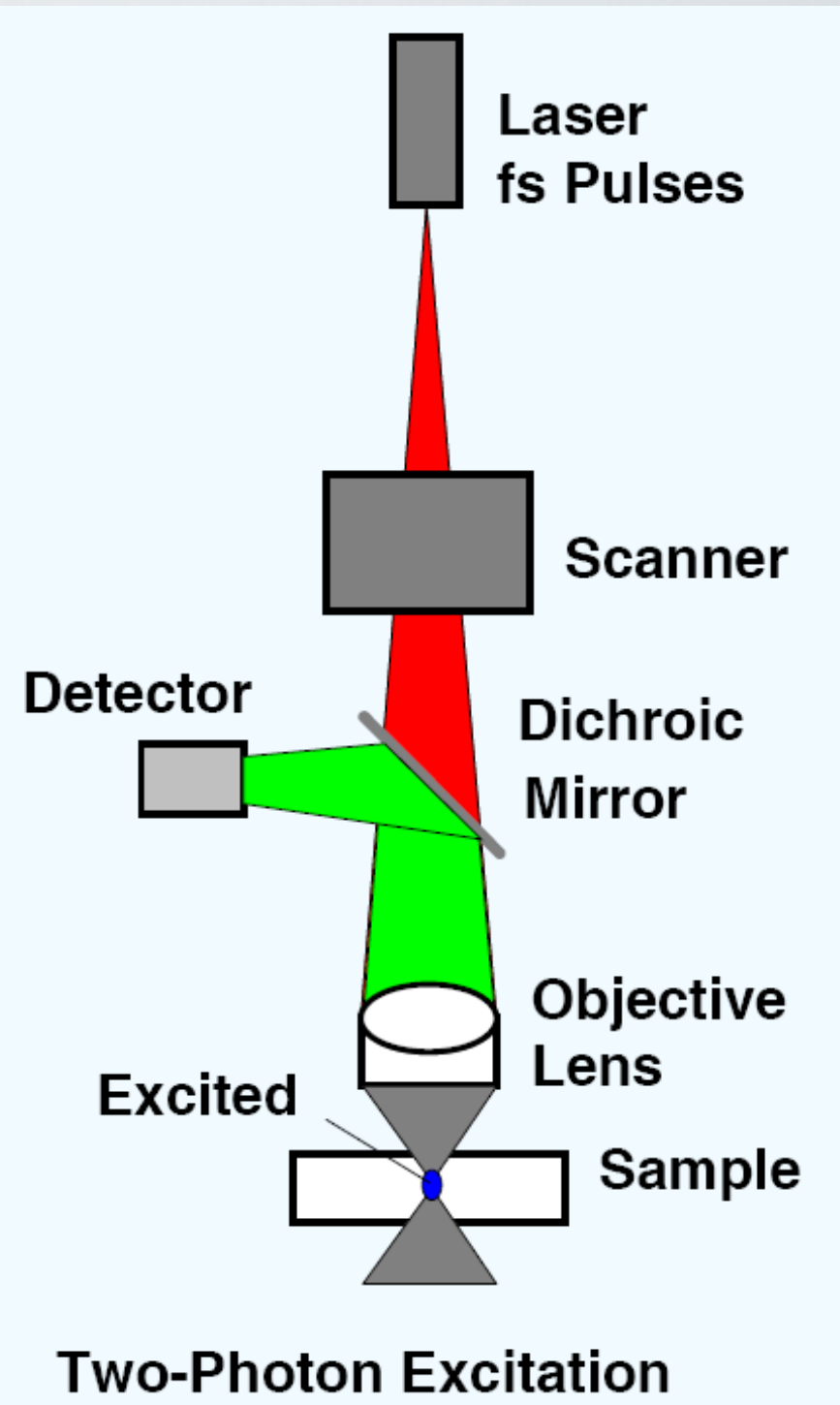
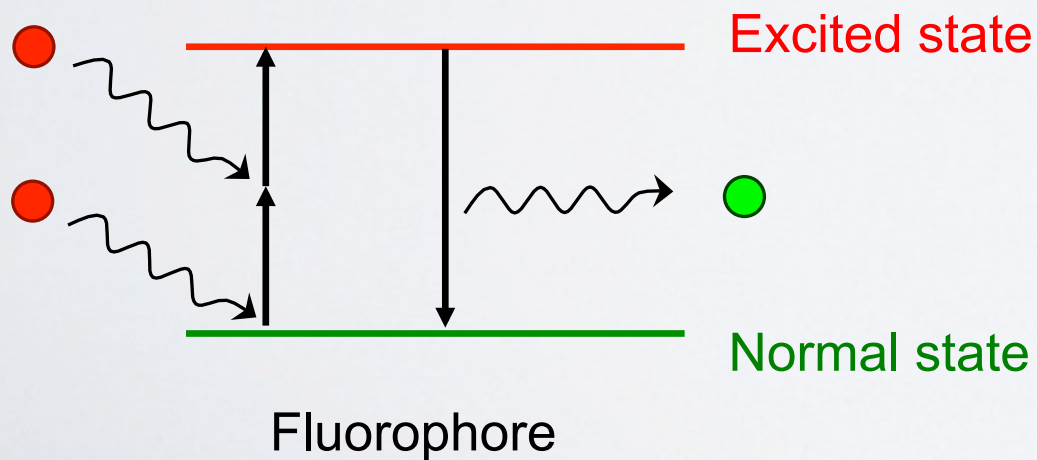


Photomultiplier Tube³

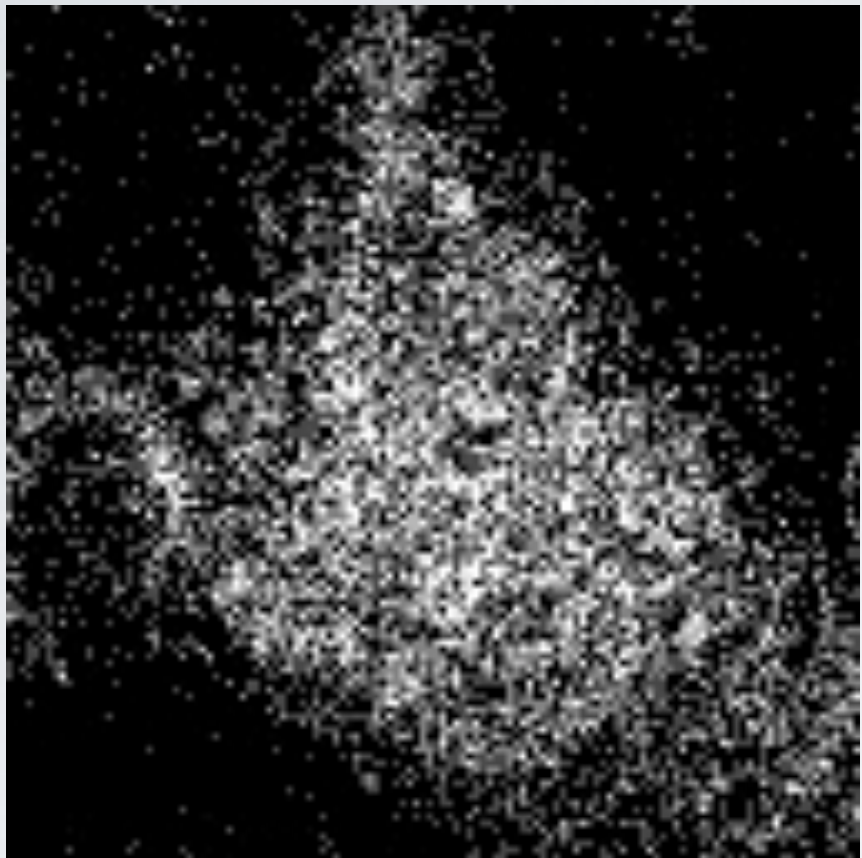
¹isuppli.com, ²edmundoptics.com, ³hamamatsu.com, ⁴sensorsinc.com, ⁵spinoff.nasa.gov

Multiphoton Fluorescence Microscopy

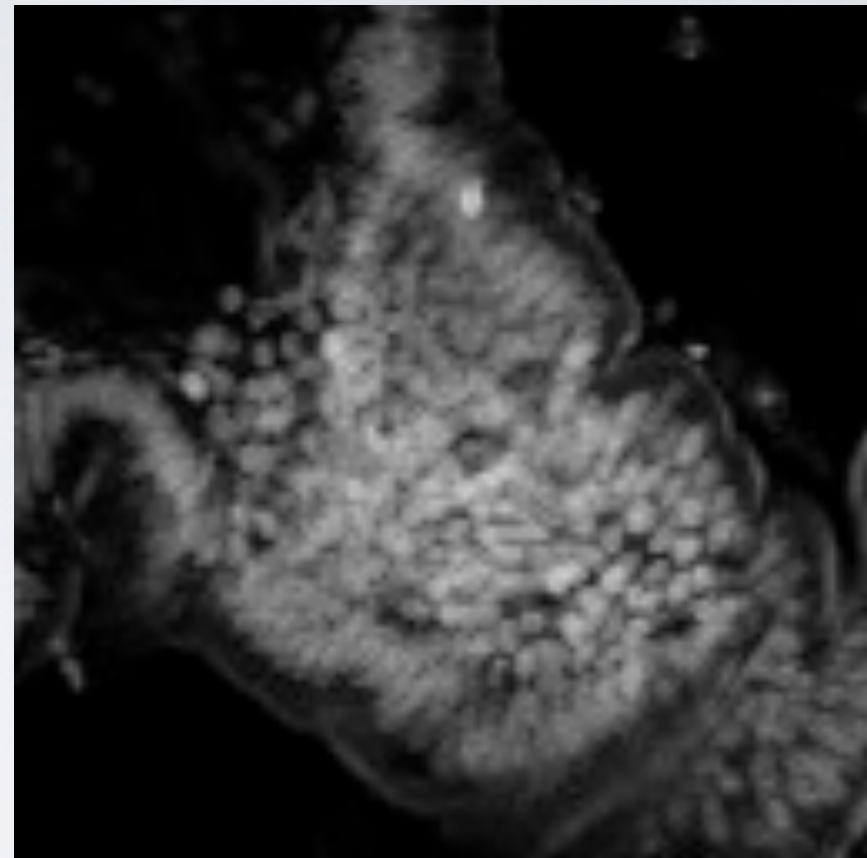
- Collaboration with LOCI group at University of Wisconsin-Madison
- High-resolution imaging of **living** specimens
- Stained with fluorescent dyes or utilize endogenous fluorophores
- **Two-photon excitation:**



Multiphoton Fluorescence Microscopy



Data: 0.1s Scan Time

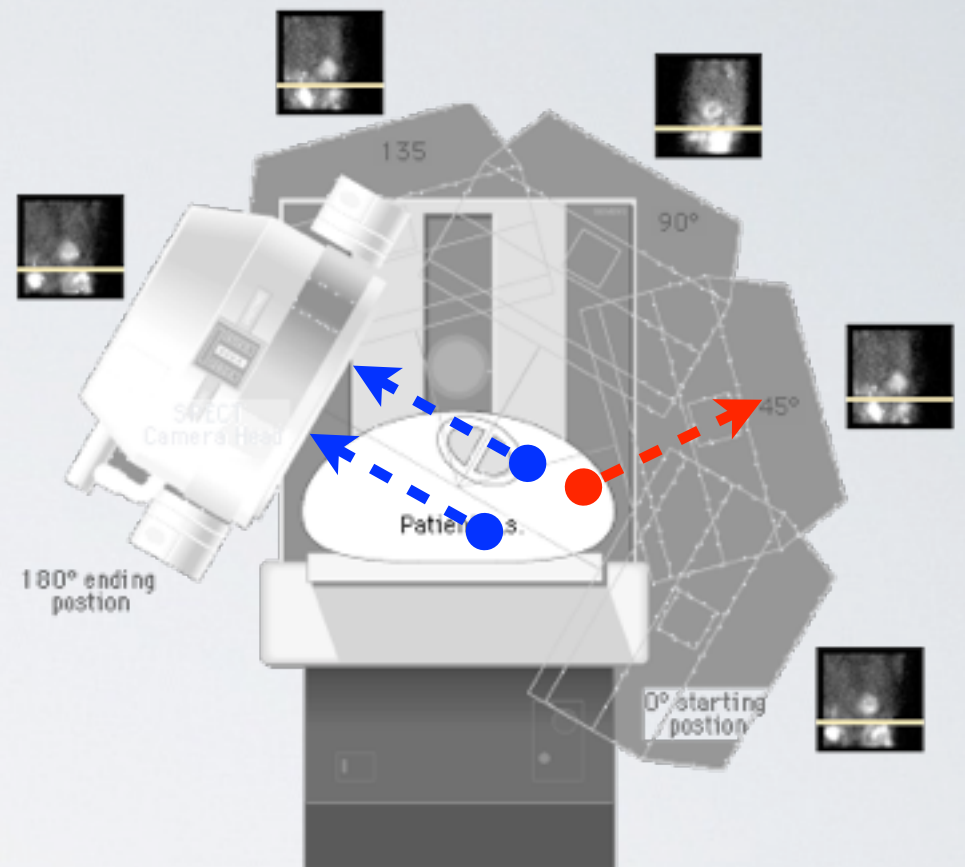


Data: 120s Scan Time

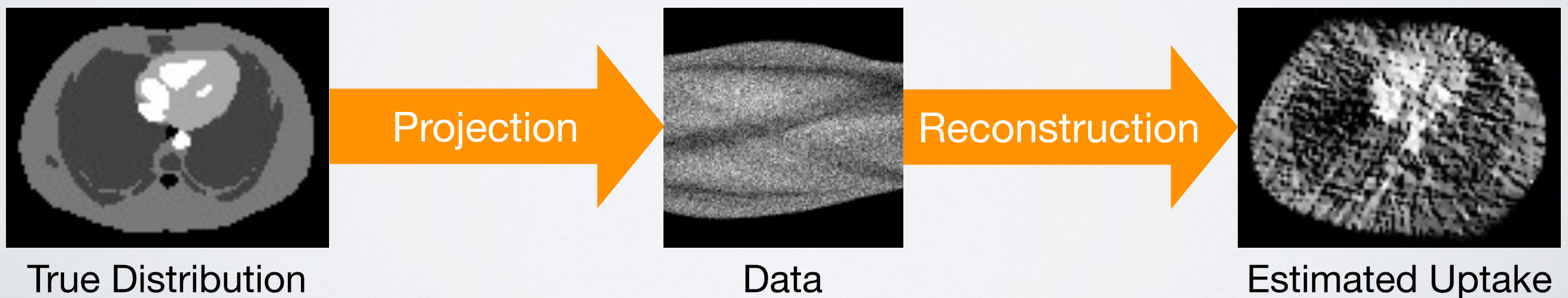
- Photon limitations:
 - Excitation laser power
 - Dwell time
- Traditional approaches:
 - Fixed binning
 - Gaussian smoothing

Single-Photon Emission Computed Tomography

- Patient injected with gamma-emitting radiopharmaceutical
- Chemical uptake inferred by measuring emitted radiation from many projection angles
- Reconstruction algorithm necessary to interpret data



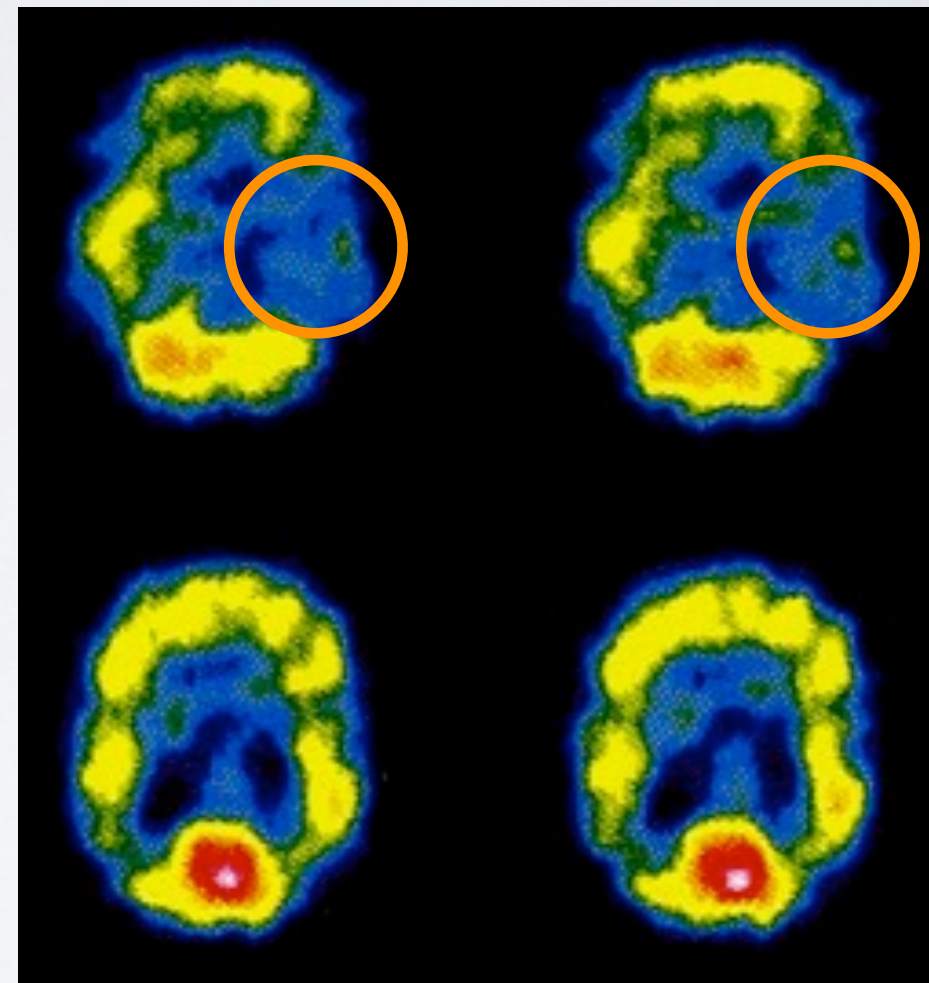
SPECT imaging camera¹



Single-Photon Emission Computed Tomography

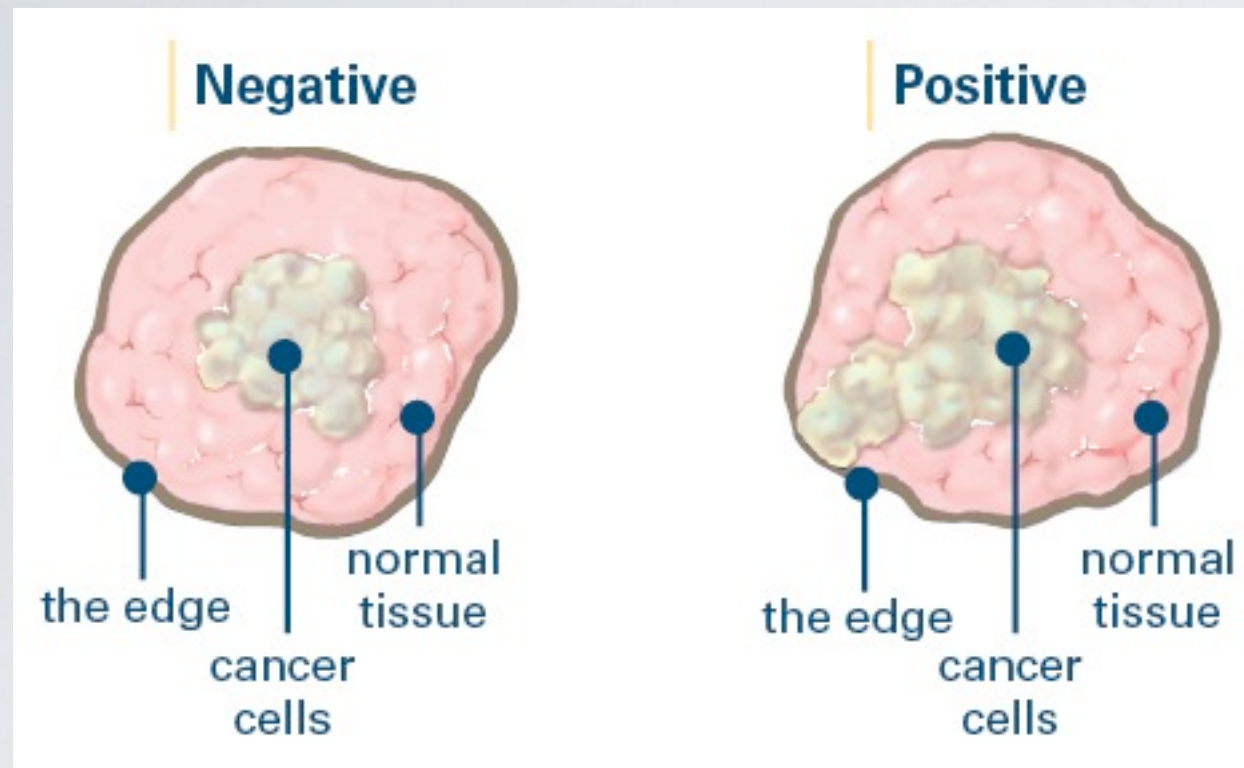
- Low-resolution images show tissue **function**
- Photon limitations:
 - Patient dose
 - Scattering and attenuation
 - Scan times

Impaired function of left temporal lobe
Source of **seizures** in patient¹



SPECT Brain Scan

Intraoperative Margin Assessment



Tumor Margin¹

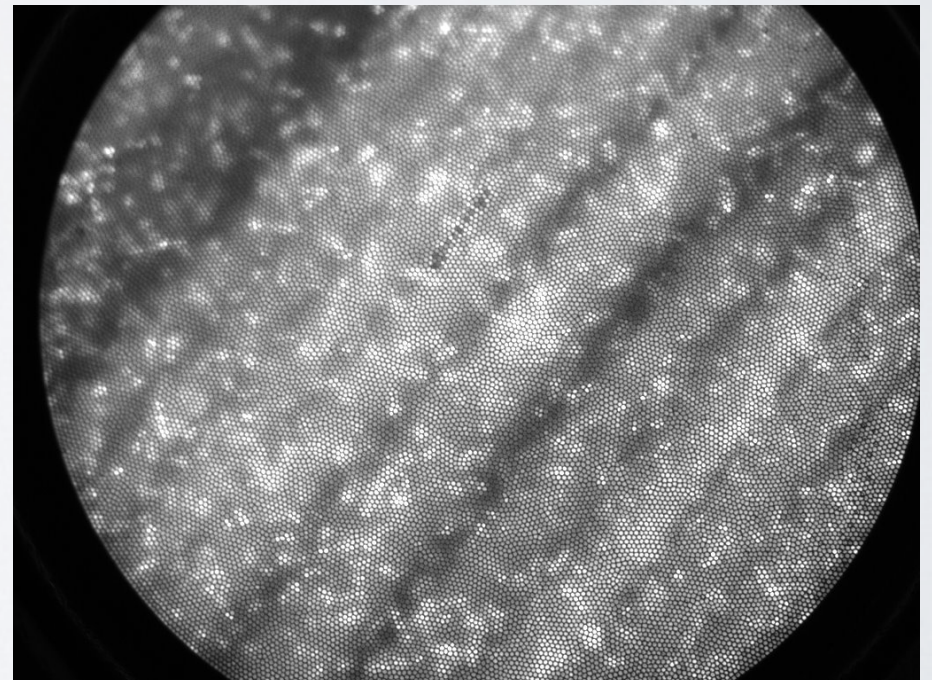
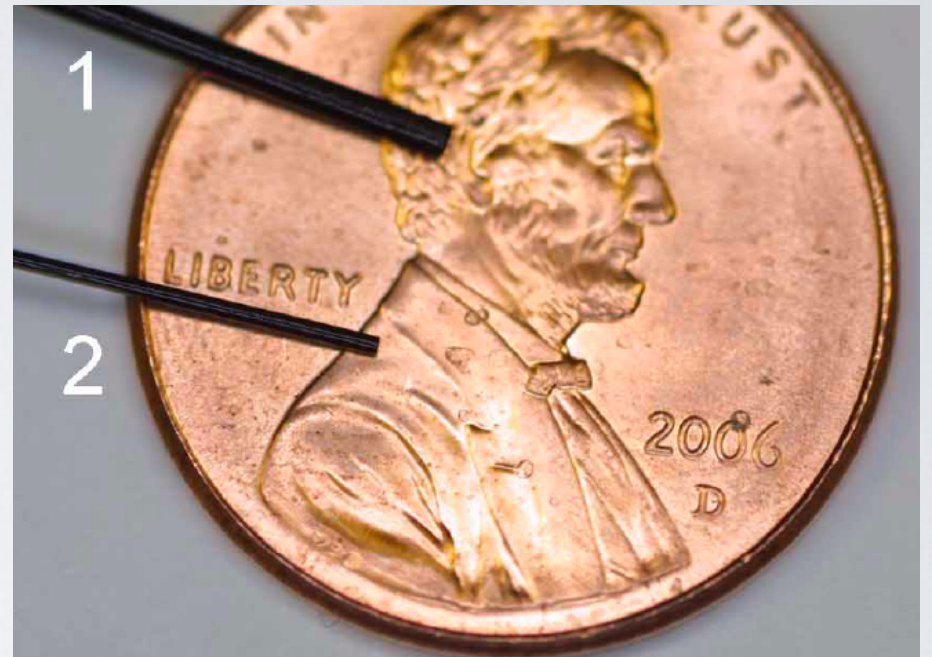
Intraoperative assessment:
Ensures complete removal
Eliminates follow-up procedures

Margin Assessment:

1. Surgically remove tumor and small **margin** of healthy tissue
2. Close the surgical incision
3. Pathologically process excised tissue
4. If margin is **positive**, patient must return for second surgery

Intraoperative Margin Assessment

- Collaboration with Prof. Ramanujam's group
- Endoscopic microscopes are a high-resolution low-cost alternative
- Uses fiberoptic bundle for confocal fluorescence imaging
- Fluorescent dyes tag key tissue structures
- Photon limitations:
 - Reduced scan time
 - Limited excitation power



Observation Model

$$y \sim \text{Poisson}(Af)$$

Nonnegative counts
 $y \in \mathbf{Z}_+^m$

Nonnegative matrix
 $A \in \mathbf{R}_+^{m \times n}$

Nonnegative intensity
 $f \in \mathbf{R}_+^n$

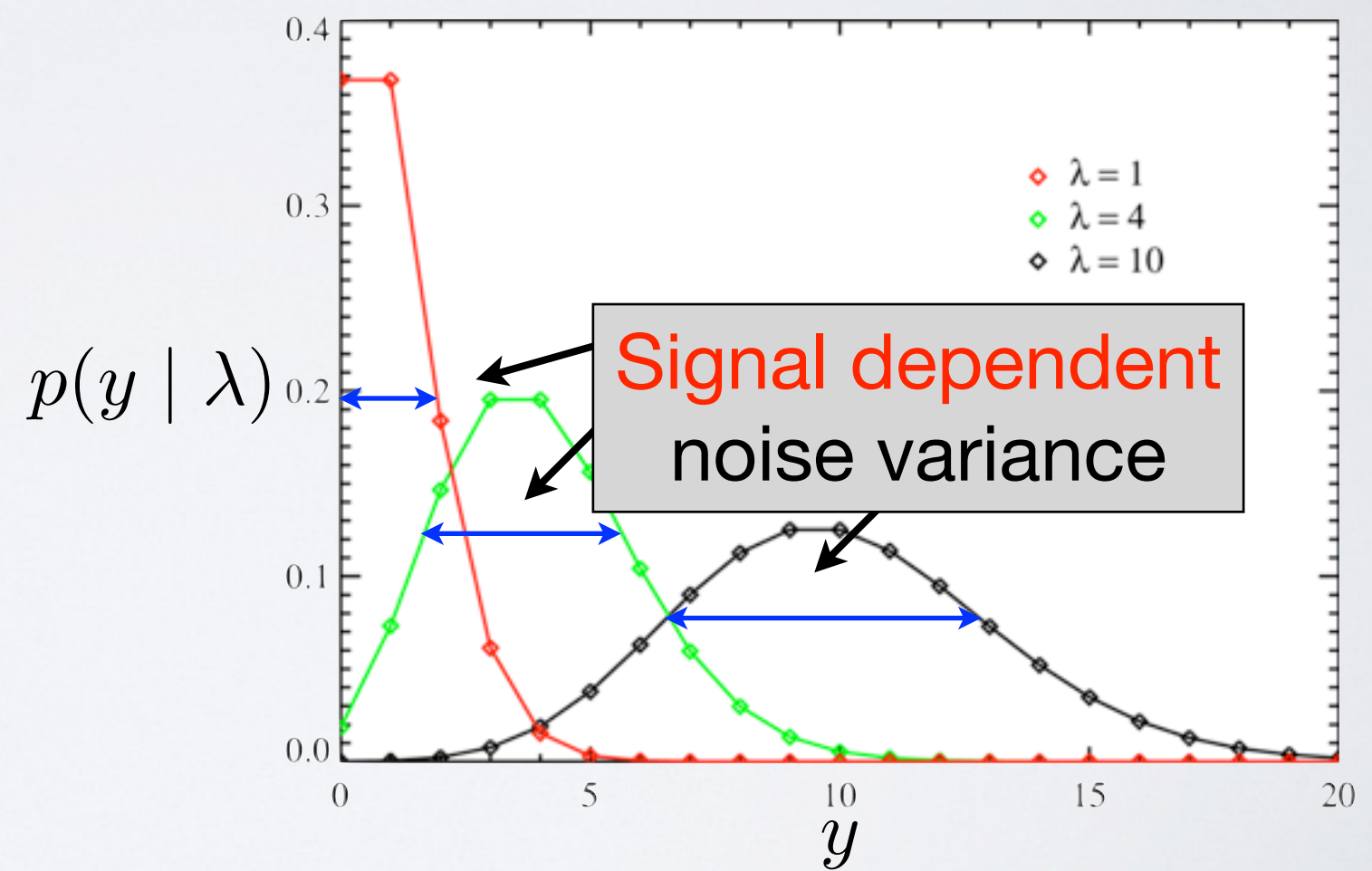
Examples:

$$\begin{aligned} A = I &\Rightarrow Af = f \\ Af &= \text{Radon}(f) \end{aligned}$$

Detector intensity
 $\lambda = Af$

Poisson distribution:

$$p(y | \lambda) = \frac{\lambda^y e^{-\lambda}}{y!}$$



Ignoring Heteroscedasticity



Truth

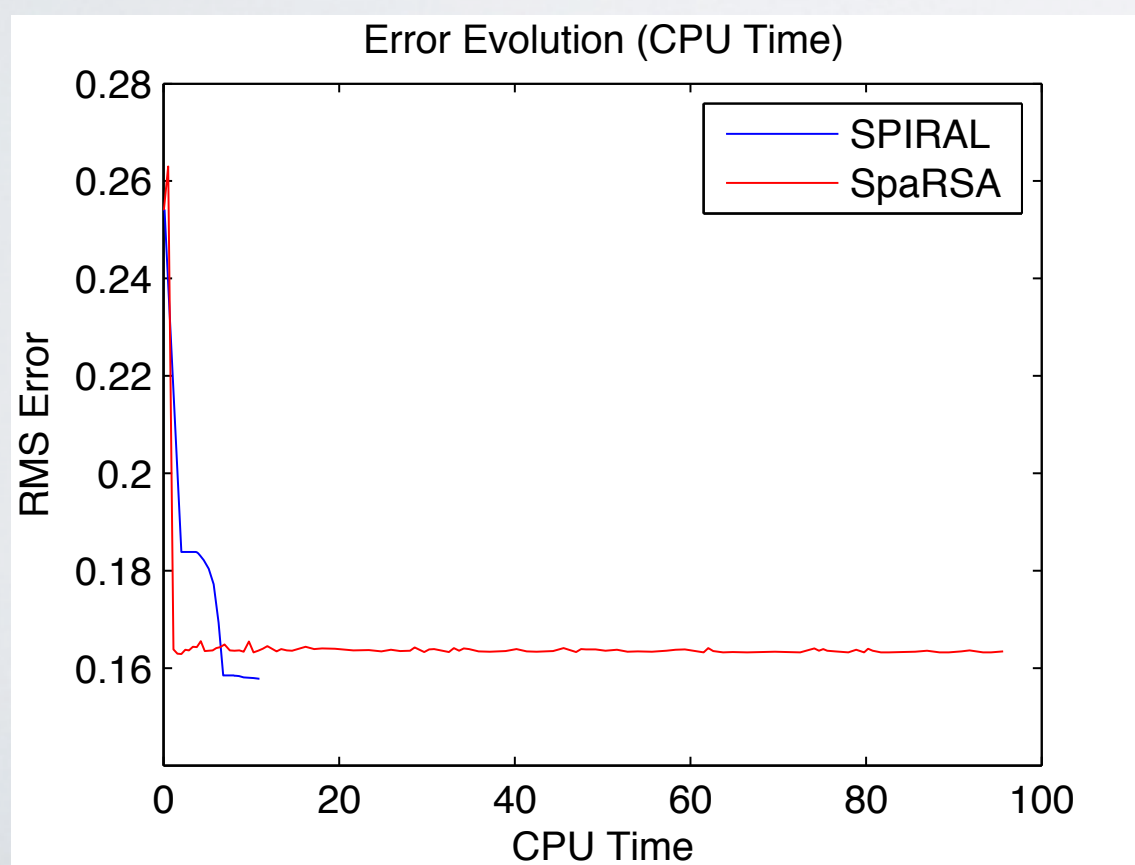
Data

SpaRSA-TV

16.34% RMSE

SPIRAL-TV

15.75% RMSE



- Simple deblurring example
- Mean photon count = 1.33
- **SPIRAL** more accurate and faster:
51 iter / 11s vs. 100 iter / 98s

Penalized Maximum Likelihood Estimation

- How do we recover signals from data?

$$\widehat{f} = \arg \min_{f \in \mathbf{R}^n} \Phi(f) := \underbrace{\sum_{i=1}^m [e_i^\top A f - y_i \log(e_i^\top A f)]}_{= \phi(f) \propto -\log p(y|Af)} + \tau \text{pen}(f)$$

subject to $f \geq 0$

Scene Model

- Challenging to optimize:

- Mindful of **nonnegativity** constraints
- Utilize **nonsmooth** penalty functions
- **Convex** objective, yet we have **singularities**

Side-Stepping Singularities

- Slight modification of data fit term:

$$\phi(f) := \sum_{i=1}^m [e_i^\top A f - y_i \log(e_i^\top A f + \beta)]$$

$\beta > 0$

- Similar assumption of known background counts¹
- Important: ϕ now Lipschitz continuously differentiable² over \mathbf{R}_+^n , meaning $\|\nabla\phi(x) - \nabla\phi(y)\|_2 \leq L\|x - y\|_2 \quad \forall x, y \in \mathbf{R}_+^n$ with

$$L \leq \frac{\max(y)}{\beta^2} \|A\|_2^2$$

¹Fessler and Erdogn (1998)

²Harmany, Marcia, and Willett (2012)

Proposed Approach

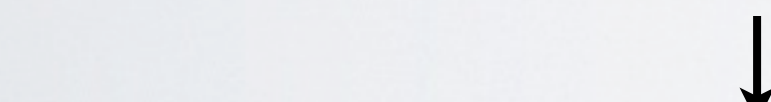
Optimization Approach:
Utilize a sequence of **quadratic approximations**

$$\phi(f) \propto -\log p(y|Af)$$

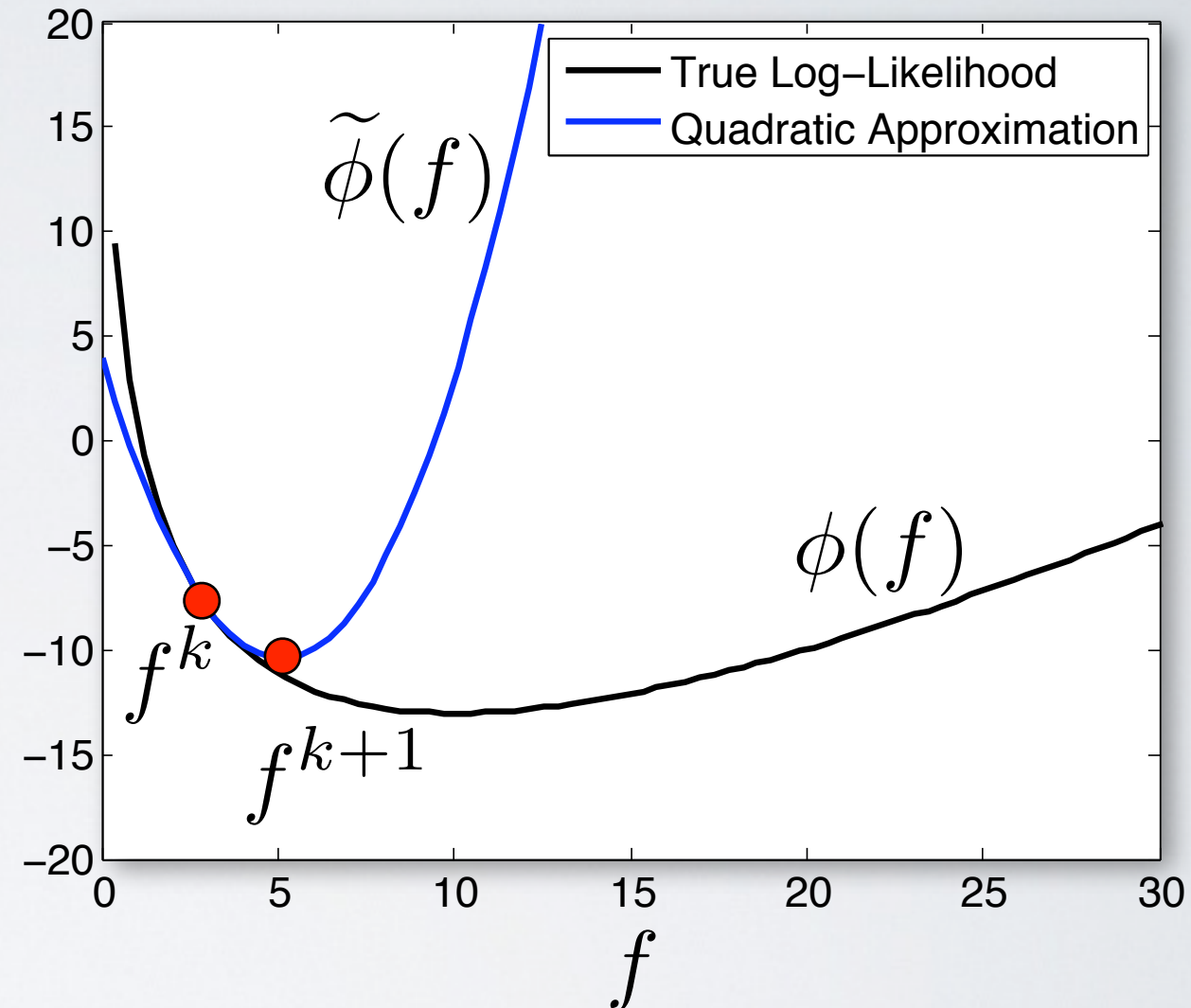
Minimization made easier by a **separable** approximation:

$$\nabla^2 \phi(f^k) \approx \alpha_k I$$

Current iterate



$$\text{Taylor: } \tilde{\phi}(f) = \phi(f^k) + \nabla \phi(f^k)^T (f - f^k) + \frac{\alpha_k}{2} \|f - f^k\|_2^2$$



Proposed Approach

Reformulate as a **denoising** problem:

$$f^{k+1} = \arg \min_f$$

$$\frac{1}{2} \|f - s^k\|_2^2 + \frac{\tau}{\alpha_k} \text{pen}(f)$$

subject to $f \geq 0$

Gradient descent step

$$s^k = f^k - \frac{1}{\alpha_k} \nabla \phi(f^k)$$

In special cases: **Analytic** solution

Related to proximal (forward-backward) splitting methods¹

In general: **No analytic solution** necessarily, however fast algorithms exist!

General Approach: **SPIRAL**²

= **S**parse **P**oisson **I**ntensity **R**econstruction **ALgori**thms

¹Combettes (2006); ²Harmany, Marcia, Willett (2009, 2012)

Sparsity Penalty (SPIRAL- ℓ_1)

$$\underset{\theta \in \mathbb{R}^n}{\text{minimize}} \quad \frac{1}{2} \|\theta - s^k\|_2^2 + \frac{\tau}{\alpha_k} \|\theta\|_1$$

Nonsmooth
Objective

subject to $W\theta \geq 0$

Transform Problem: $\theta = u - v, u \geq 0, v \geq 0$

$$\underset{(u,v) \in \mathbb{R}^{2n}}{\text{minimize}} \quad \frac{1}{2} \|u - v - s^k\|_2^2 + \frac{\tau}{\alpha_k} \mathbf{1}^T(u + v)$$

Smooth
Objective

subject to $u \geq 0, v \geq 0, W(u - v) \geq 0$

Difficult
Constraints

Lagrangian Dual Formulation (zero duality gap):

$$\underset{(\lambda, \gamma) \in \mathbb{R}^{2n}}{\text{minimize}} \quad \frac{1}{2} \|s^k + \gamma + W^T \lambda\|_2^2 - \|s^k\|_2^2$$

Smooth
Objective

subject to $\lambda \geq 0, \frac{-\tau}{\alpha_k} \mathbf{1} \leq \gamma \leq \frac{\tau}{\alpha_k} \mathbf{1}$

Simple (bound)
Constraints

Next Primal Iterate: $\theta^{k+1} = s^k + \gamma^\star + W^T \lambda^\star$

Sparsity Penalty (SPIRAL- ℓ_1)

$$\underset{(\lambda, \gamma) \in \mathbb{R}^{2n}}{\text{minimize}} \quad \frac{1}{2} \|s^k + \gamma + W^T \lambda\|_2^2 - \|s^k\|_2^2$$

$$\text{subject to} \quad \lambda \geq 0, \frac{-\tau}{\alpha_k} \mathbb{1} \leq \gamma \leq \frac{\tau}{\alpha_k} \mathbb{1}$$

Solve via **Alternating Minimization**:

$$\gamma^{(j)} = \text{mid} \left\{ \frac{-\tau}{\alpha_k} \mathbb{1}, -s^k - W^T \lambda^{(j-1)}, \frac{\tau}{\alpha_k} \mathbb{1} \right\}$$

$$\lambda^{(j)} = \left[-W(s^k + \gamma^{(j)}) \right]_+$$

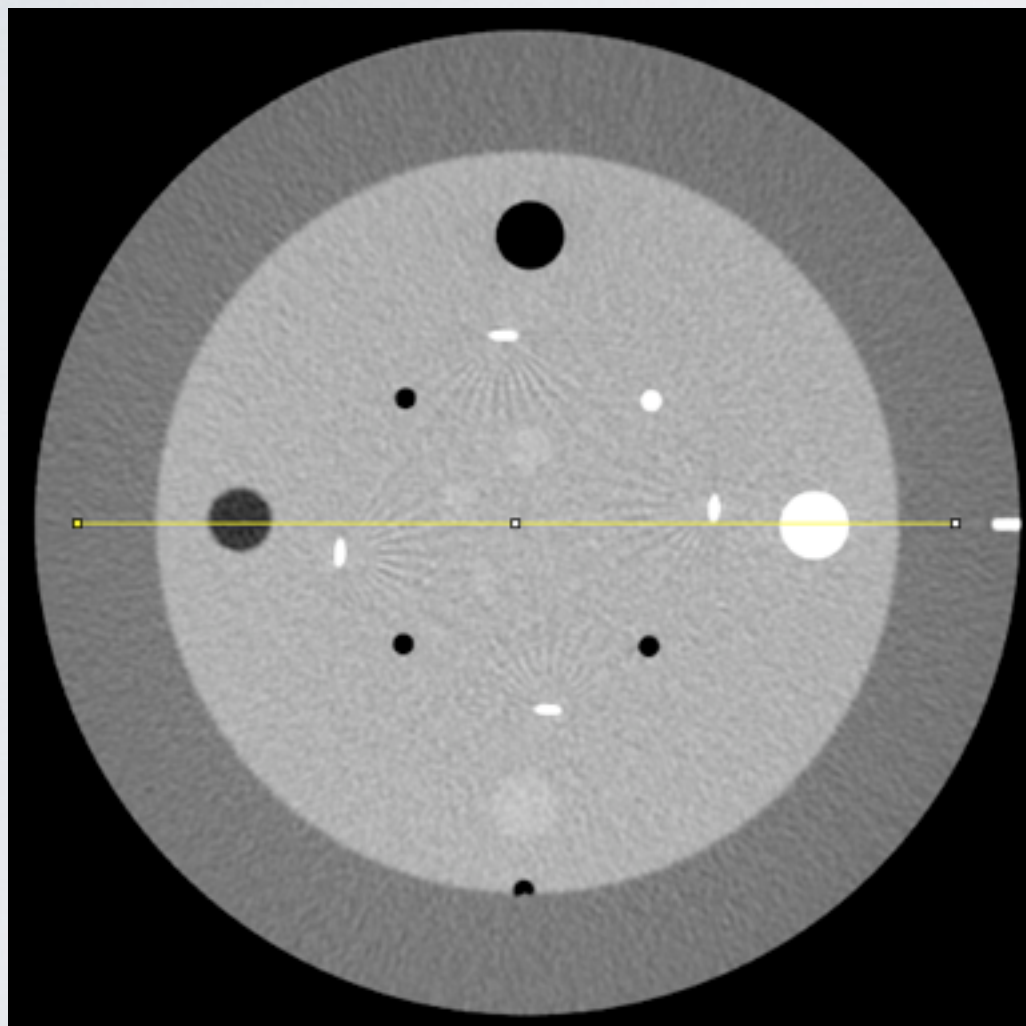
Property: Guaranteed Primal **Feasibility**

$$\begin{aligned} W\theta^{(j)} &= Ws^k + W\gamma^{(j)} + \lambda^{(j)} \\ &= \left[W(s^k + \gamma^{(j)}) \right]_+ \geq 0 \end{aligned}$$

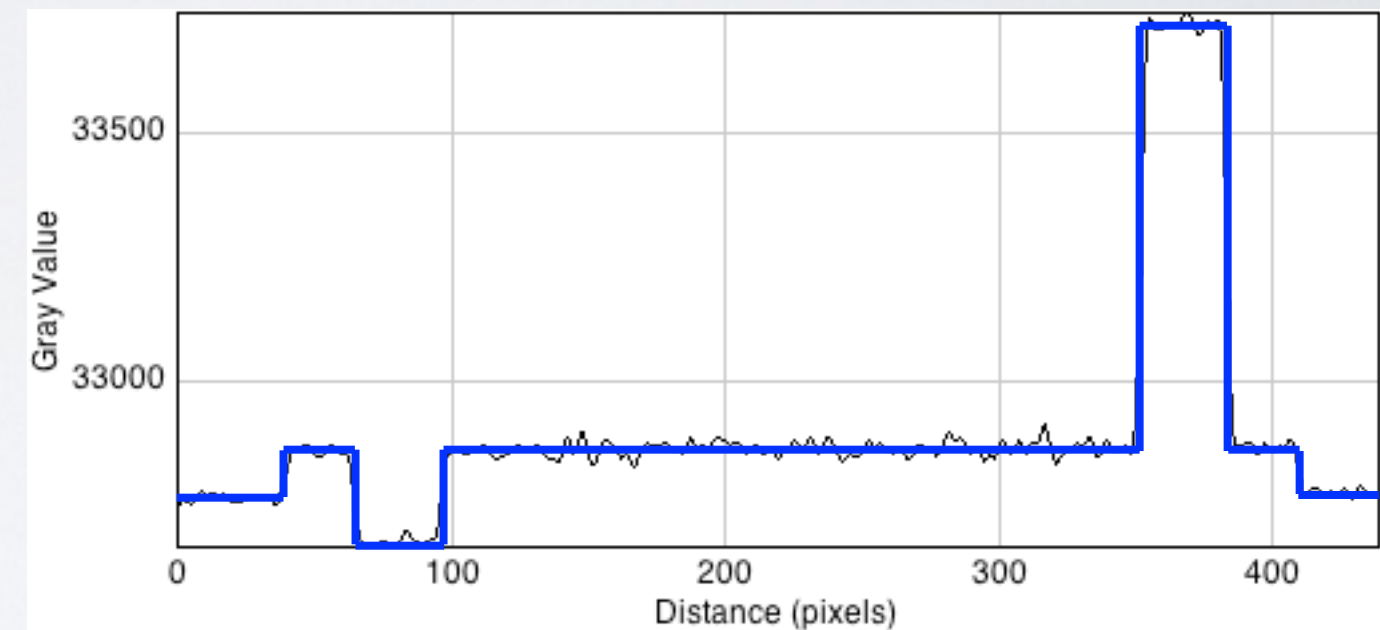
Early Termination Always Feasible!

Total Variation Regularization

Example: CT Phantom



Noise in image yields **high TV**



Smoothing in homogenous regions yields **low TV**

SPIRAL-TV

Use TV seminorm in SPIRAL iteration:

$$f^{k+1} = \arg \min_f \frac{1}{2} \|f - s^k\|_2^2 + \frac{\tau}{\alpha_k} \|f\|_{\text{TV}}$$

subject to $f \geq 0$

Special case of convex-constrained TV-penalized deblurring
(constraint set = \mathbb{R}_+^n , blur = δ)

Solvable using the FISTA algorithm¹

¹Beck, Teboulle (2009)

SPIRAL

Simplified Pseudocode:

Algorithm SPIRAL

- 1: **Initialize** Choose initial solution f^0 and regularization τ .
Start iteration counter $k \leftarrow 0$.
- 2: **repeat**
- 3: Choose stepsize parameter α_k ← **Flexibility in choice**
- 4: Compute $s^k = f^k - \frac{1}{\alpha_k} \nabla \phi(f^k)$
- 5: $f^{k+1} \leftarrow$ nonnegative denosing of s^k with regularization $\frac{\tau}{\alpha_k}$
- 6: $k \leftarrow k + 1$
- 7: **until** Stopping criterion is satisfied

Convergence Result

- Three mild assumptions:
 - On fidelity: ϕ is convex and Lipschitz continuously differentiable on \mathbf{R}_+^n
 - On penalty: pen is convex and continuous on \mathbf{R}_+^n
 - Together: $\Phi = \phi + \tau \text{pen}$ is coercive ($\lim_{\|f\|_2 \rightarrow \infty} \Phi(f) = +\infty$)
- **Theorem:** SPIRAL converges to a minimizer of Φ , and the sequence of objective values converges sublinearly:

$$\Phi(f^k) - \Phi(\hat{f}) \leq \frac{c}{k}$$

If ϕ is strongly convex, then the objective converges R -linearly:

$$\Phi(f^k) - \Phi(\hat{f}) \leq Cr^k(\Phi(f^0) - \Phi(\hat{f}))$$

for some $r \in (0, 1)$

Comparison to Other Methods

- Richardson-Lucy deconvolution methods known to exhibit **slow** convergence (multiplicative update)
- Variance stabilizing (Anscombe) transforms require sufficiently **high** photon counts, limited use in inverse problems
- Complete-data EM algorithms are memory **inefficient**: $O(nm)$
- Many Poisson TV **denoising** methods do not extend to inverse problem settings
- Approaches based on augmented Lagrangians (ADMM, split Bregman) require a matrix inverse involving $A^T A$, generally difficult outside of **deconvolution**

Dey et al. (2004); Le et al. (2007); Figueiredo et al. (2006); Beck, Teboulle (2009);
Figueiredo, Bioucas-Dias (2010); Dupe et al. (2009)

Alternating Direction Method of Multipliers

PIDAL: Poisson Image Deconvolution by AL¹

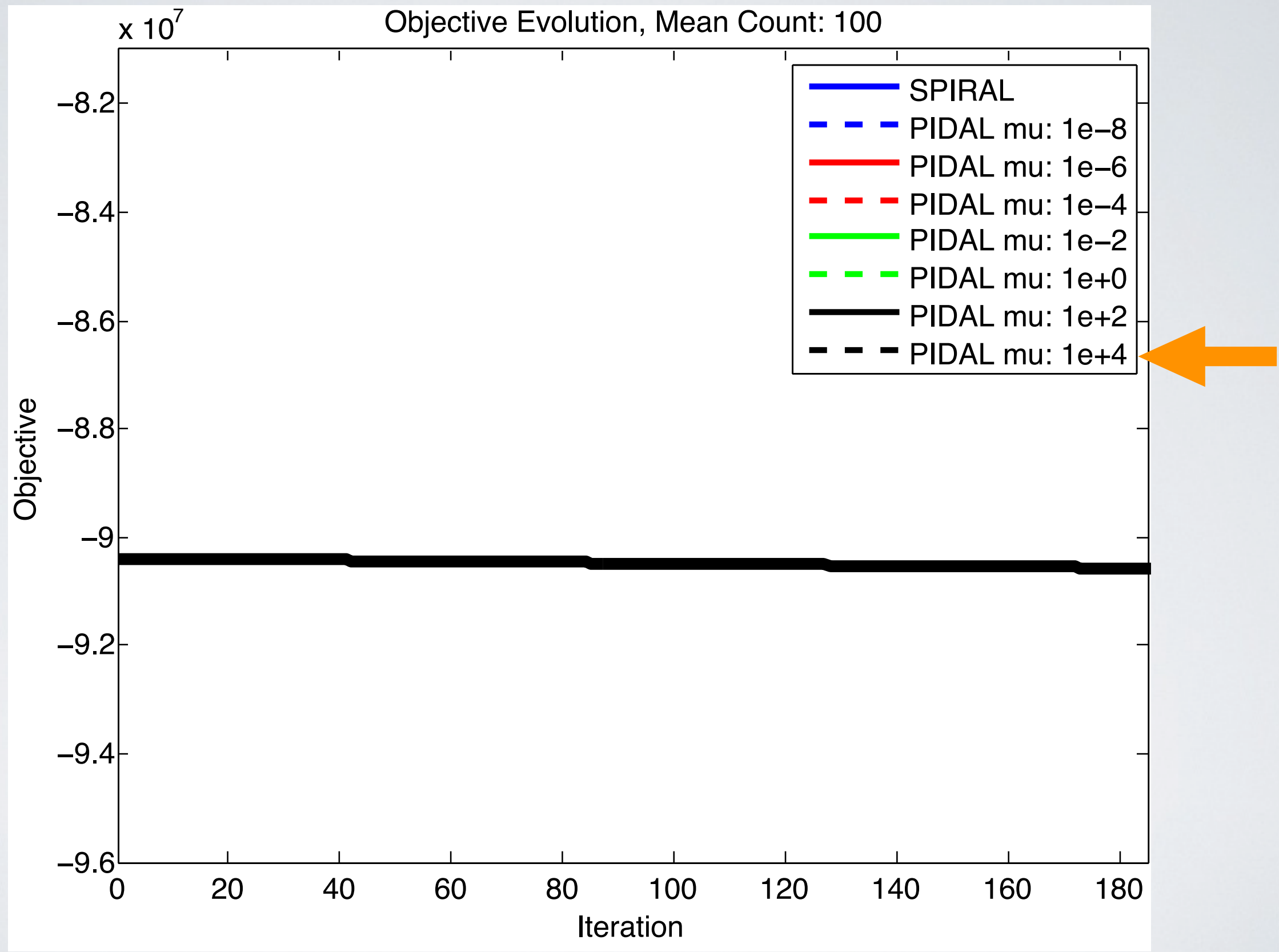
$$L_\mu(f, u, v, \lambda_u, \lambda_v) = -\log p(y|u) + \tau \text{pen}(v) + \delta_+(u) \leftarrow \boxed{\text{Objective}}$$
$$+ \lambda_u^\top (Af - u) + \lambda_v^\top (f - v) \leftarrow \boxed{\text{Lagrangian}}$$
$$+ \frac{\mu}{2} \|Af - u\|_2^2 + \frac{\mu}{2} \|f - v\|_2^2 \leftarrow \boxed{\text{Augmentation}}$$

Proper selection crucial!

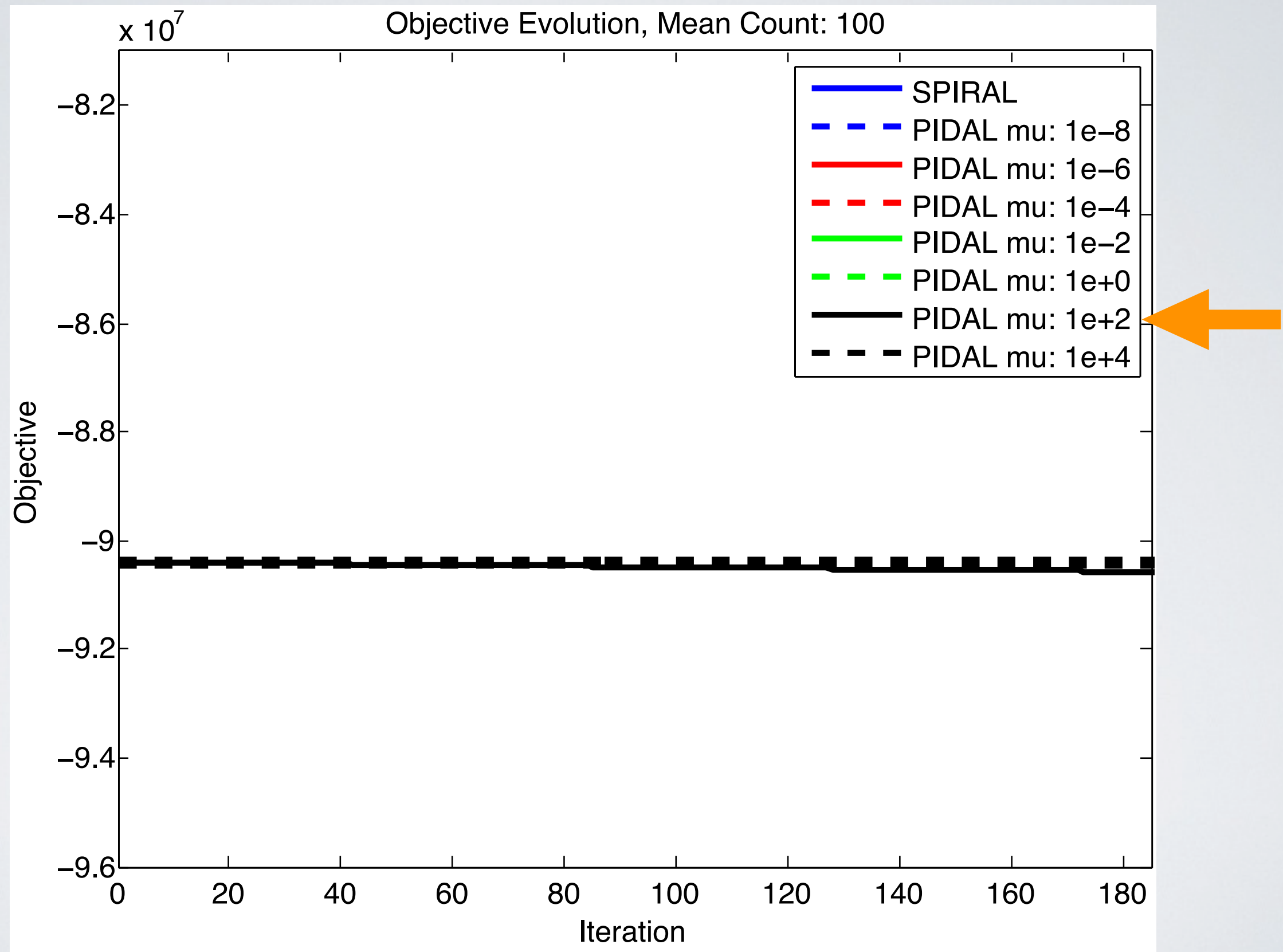
The diagram illustrates the PIDAL objective function. It is composed of three main parts: an Objective term, a Lagrangian term, and an Augmentation term. The Augmentation term contains two specific terms that are highlighted with orange circles. Arrows from these circled terms point to a box at the bottom that emphasizes the importance of proper selection.

- Algorithm: Alternating minimization followed by multiplier update
- Challenges: Selecting μ , computing $(A^\top A + I)^{-1}$

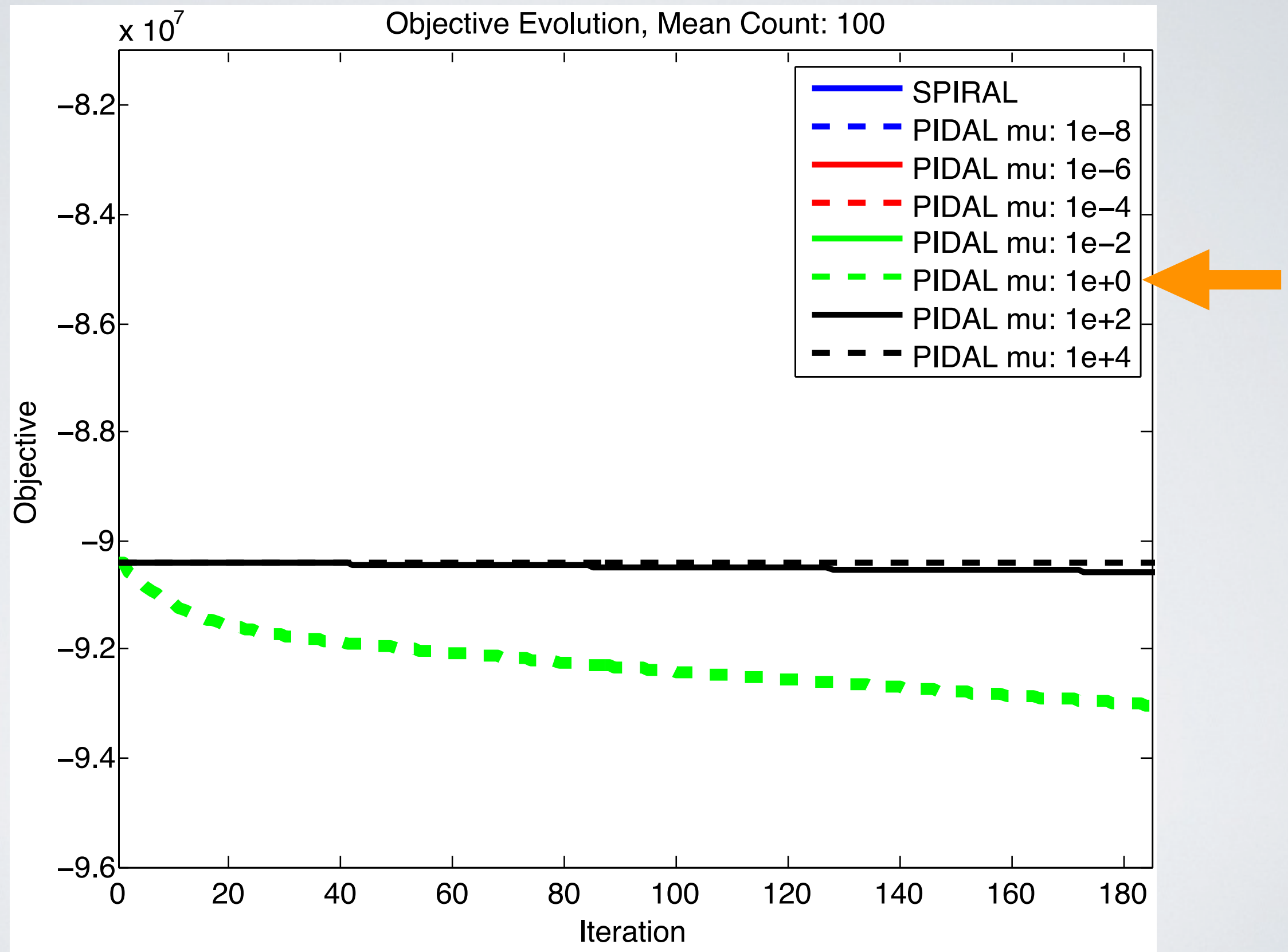
ADMM in Practice



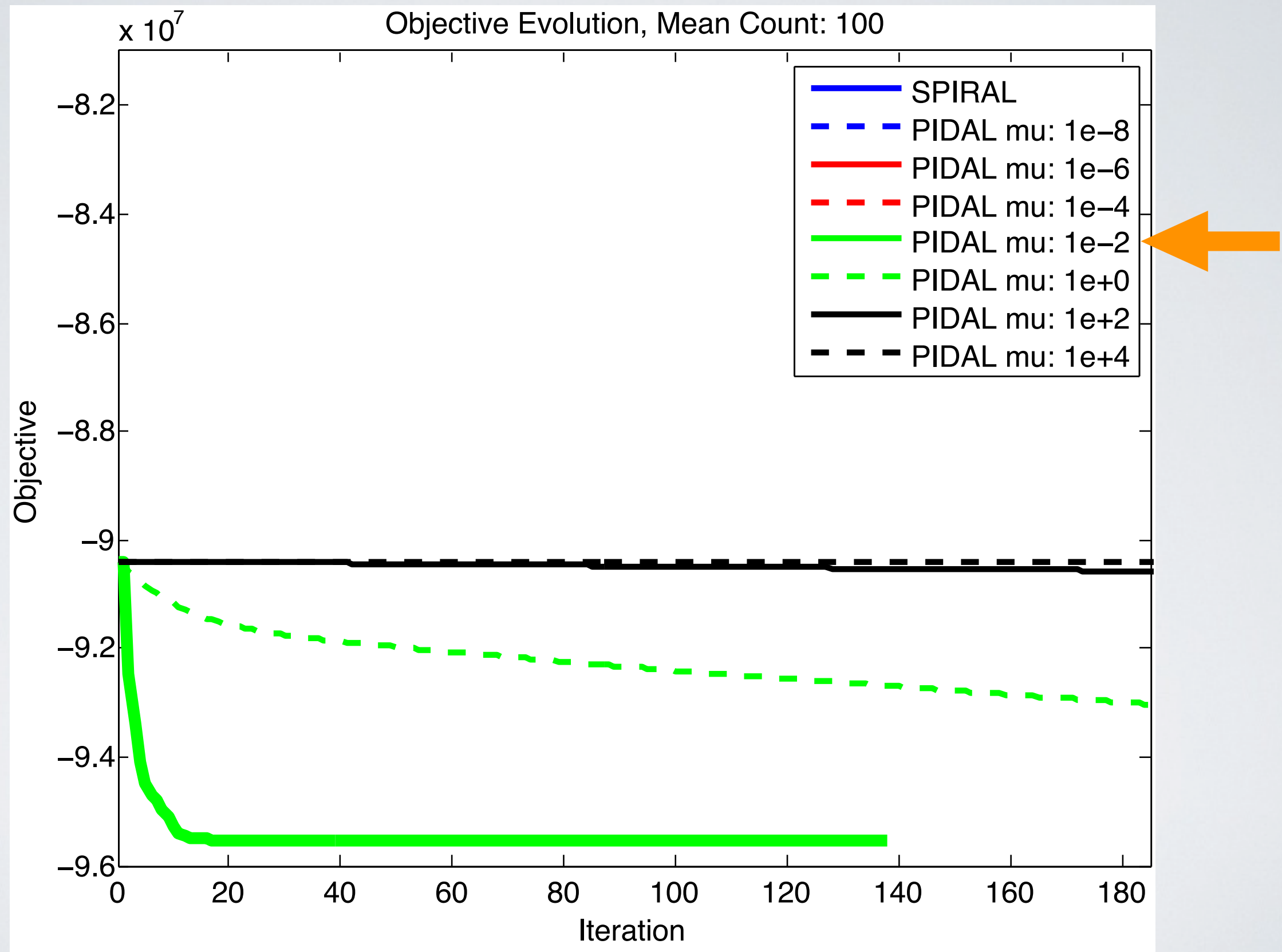
ADMM in Practice



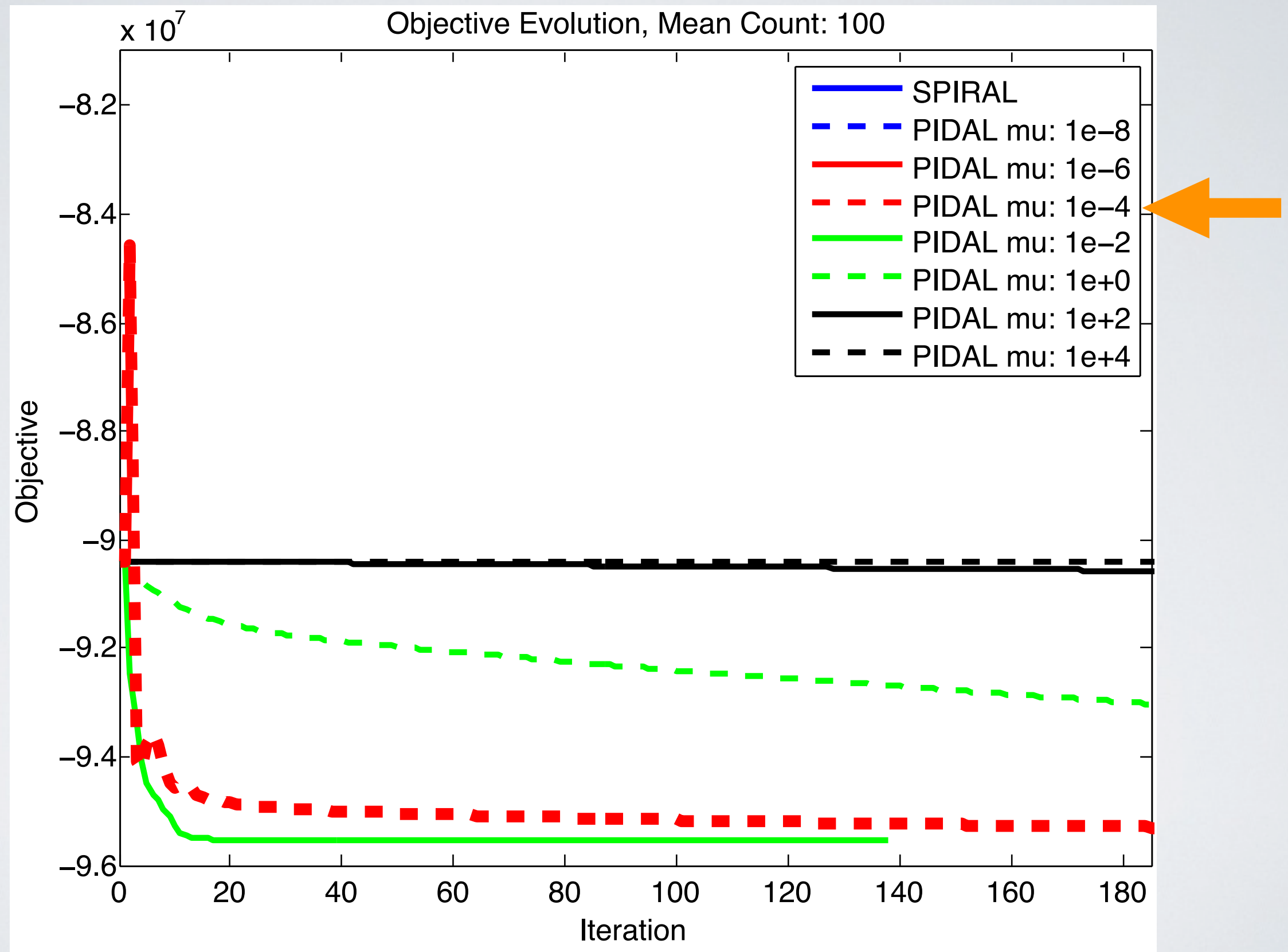
ADMM in Practice



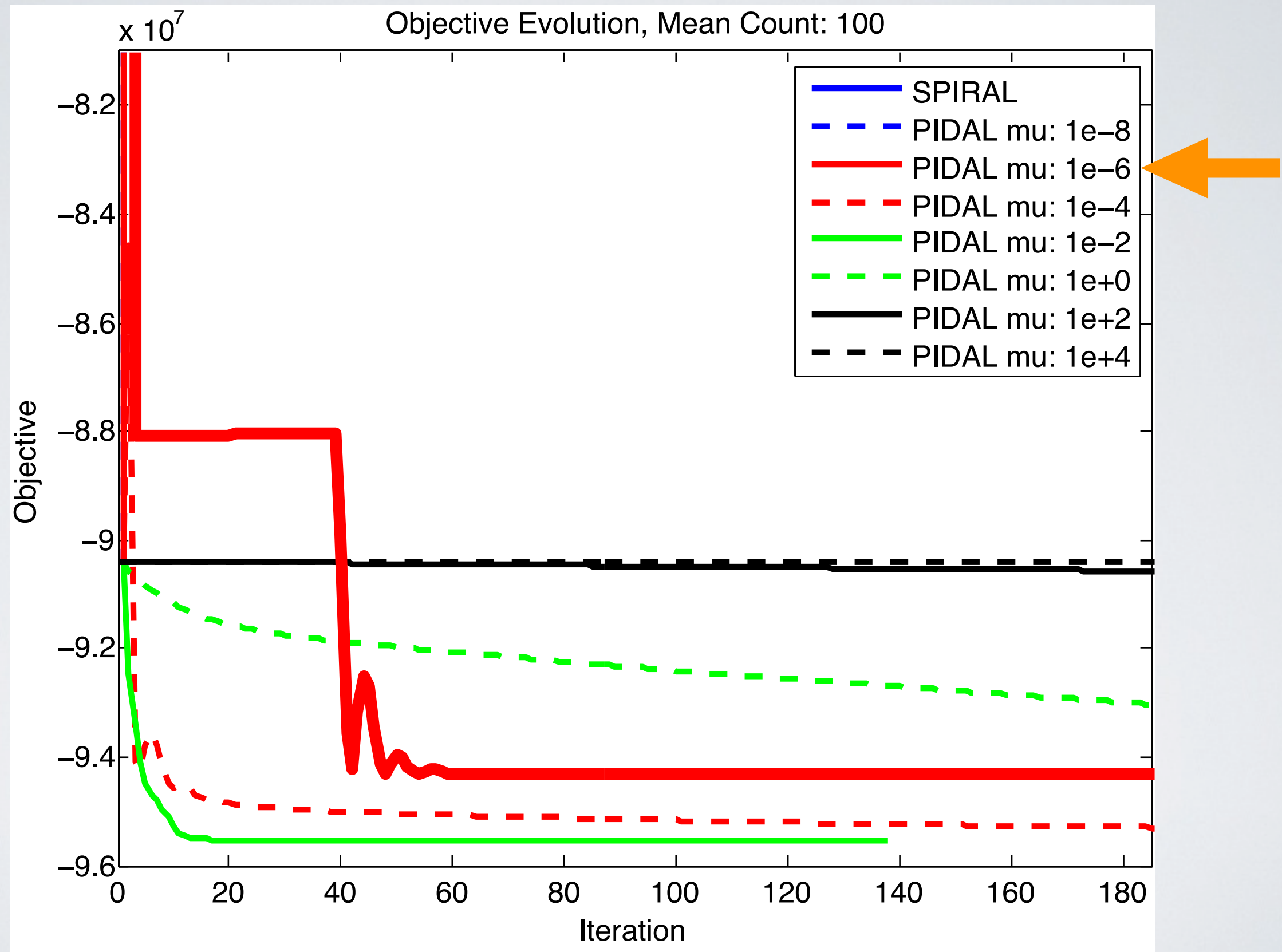
ADMM in Practice



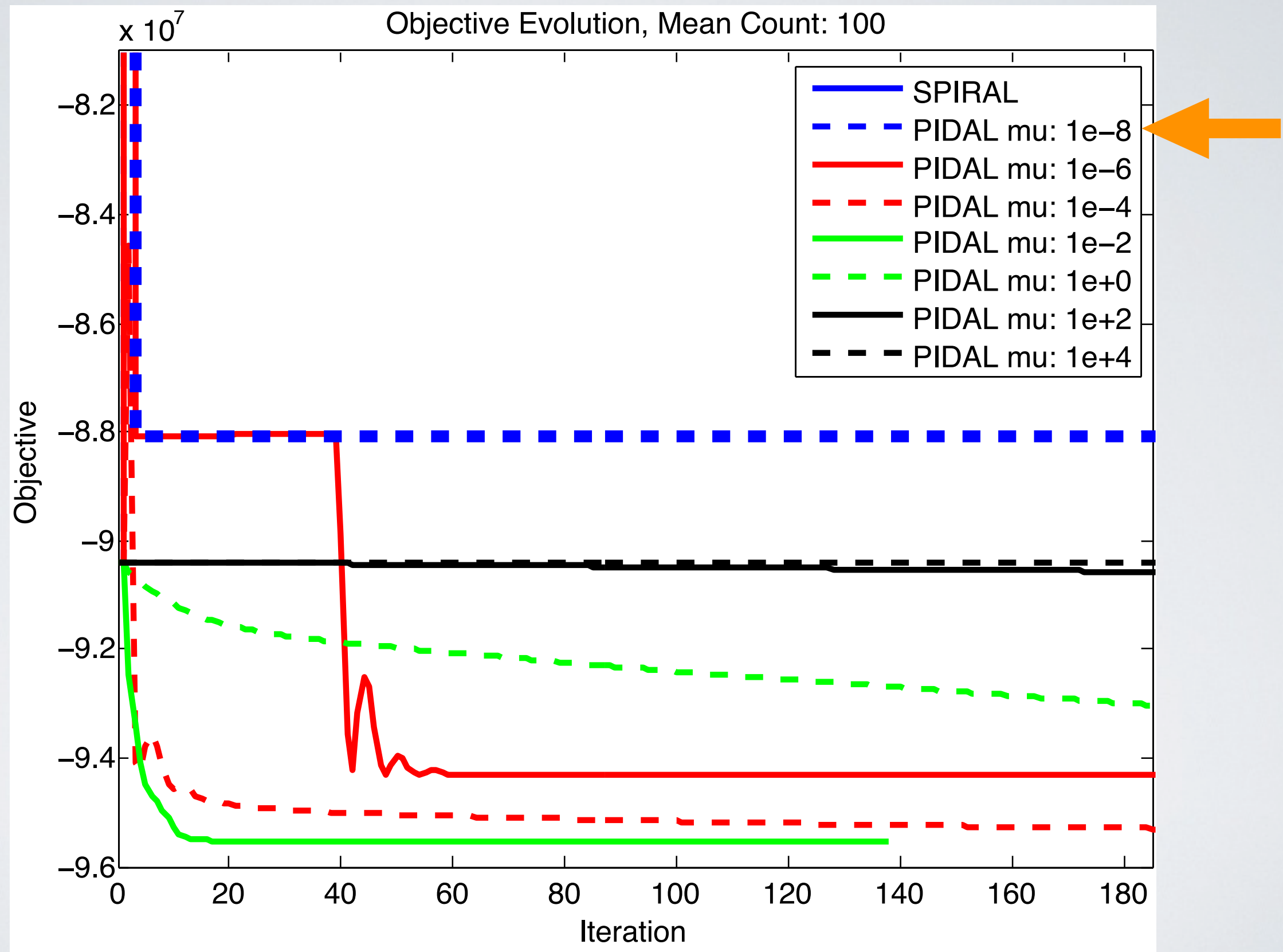
ADMM in Practice



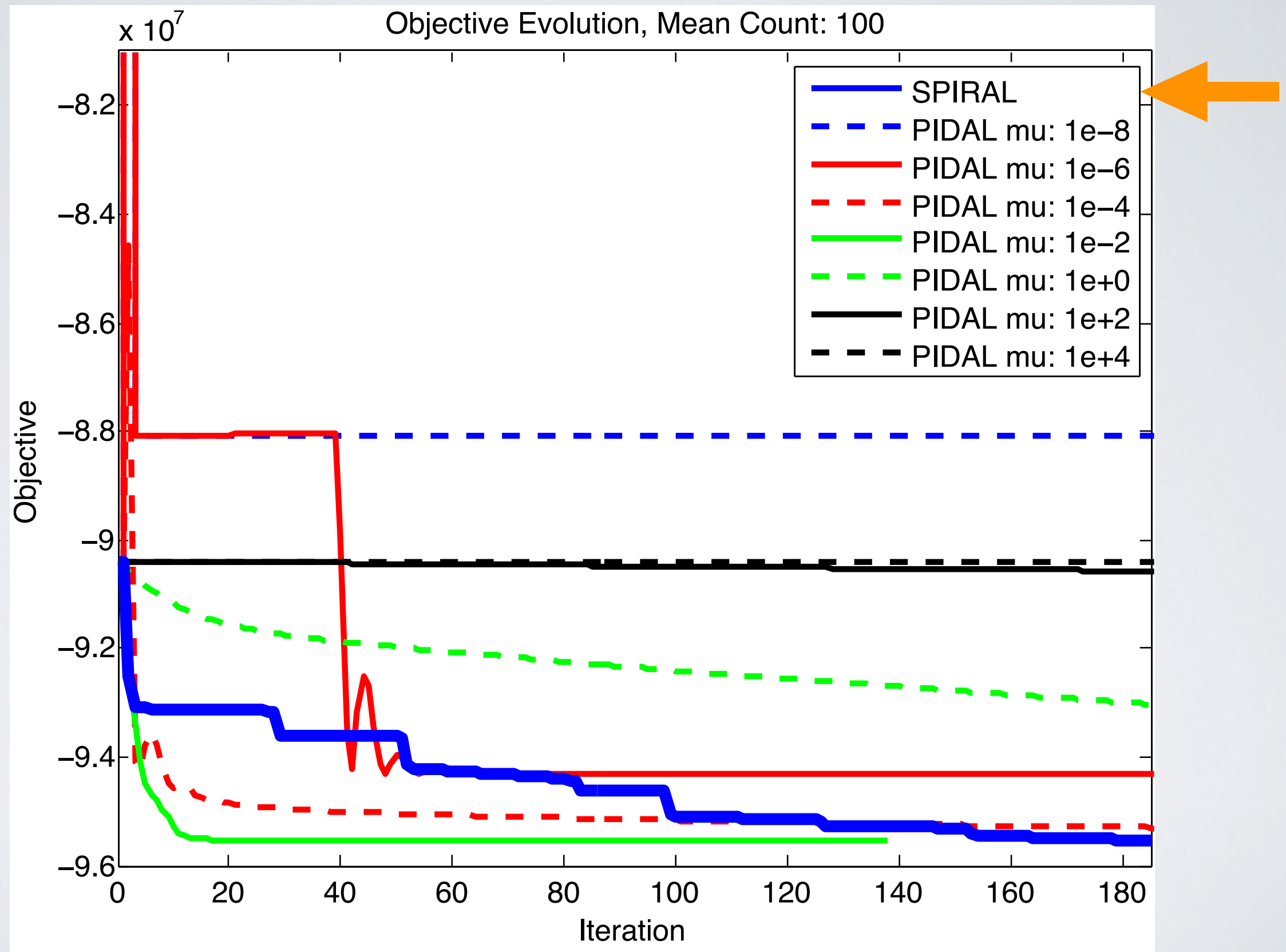
ADMM in Practice



ADMM in Practice



ADMM in Practice



SPIRAL in Action

- Applicable to a wide variety of estimation tasks
 - Poisson Compressed Sensing
 - Multiphoton fluorescent microscopy
 - Dictionary learning in Poisson noise
 - Sparse Decomposition for Margin Assessment
- SPIRAL plays a crucial role in each of these areas

Poisson Compressed Sensing

- CS: Design imaging hardware to minimize measurements

$$\textcolor{red}{m} = O(s \log n)$$

- Good: measurements costly
- Apply to optical imaging?

- Problem constraints:

Hardware can only aggregate

$$A_{i,j} \geq 0$$

Intensity preservation

$$\sum_{i=1}^n (Af)_i \leq \sum_{j=1}^n f_j = I$$

Theoretical Performance Bound¹

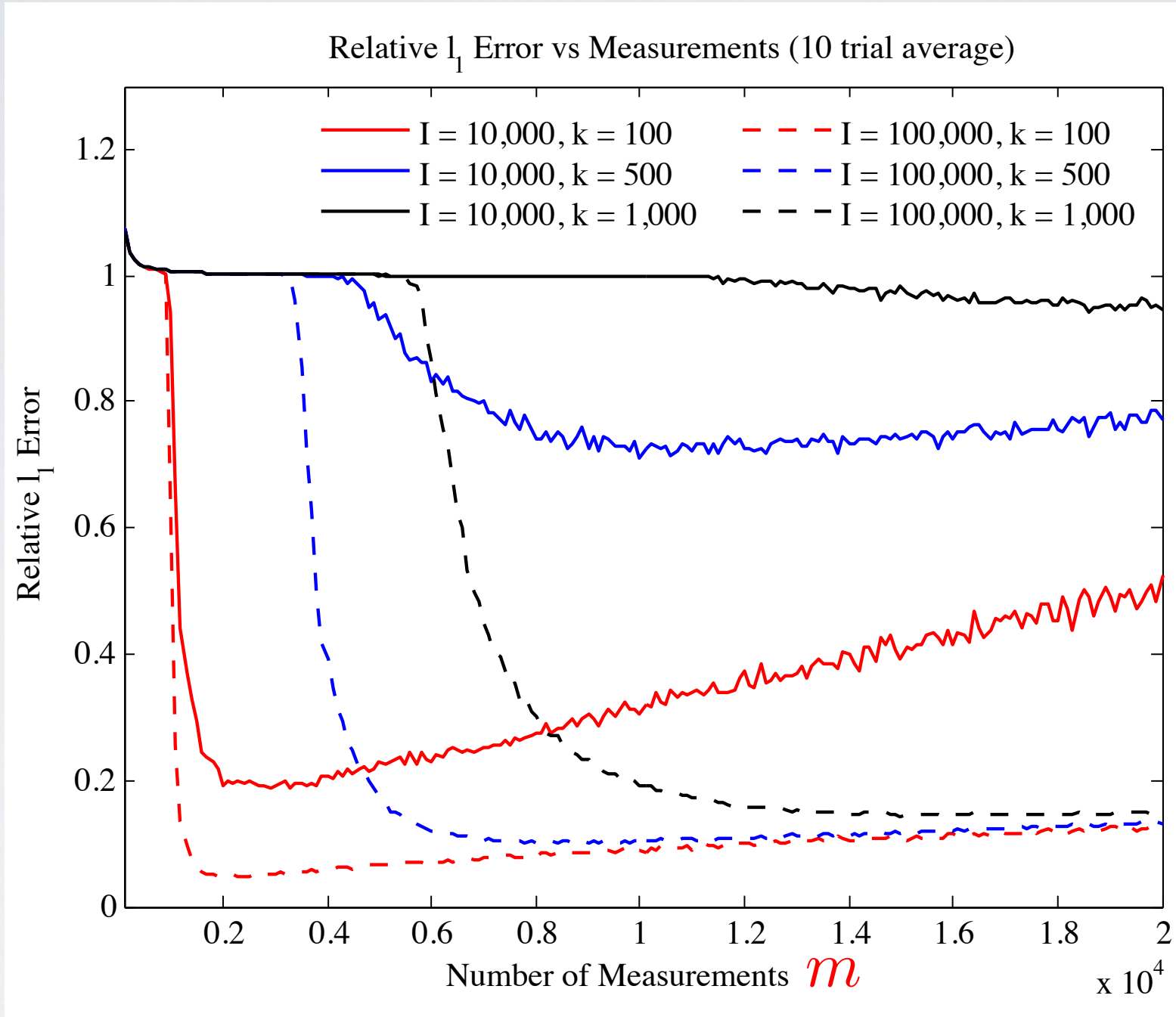
$$\mathbf{E} \left[\frac{\|\hat{f} - f\|_1}{I} \right] = O \left[\textcolor{red}{m} \left(\frac{\log n}{I} \right)^{\frac{2\alpha}{(2\alpha+1)}} + \frac{\log(n/\textcolor{red}{m})}{m} \right]$$

- Too few: insufficient diversity

- Too many: insufficient signal

¹Raginsky, Sina, Harmany, Marcia, Willett, and Calderbank (2011)

Poisson Compressed Sensing



$$\mathbf{E} \left[\frac{\|\hat{f} - f\|_1}{I} \right] = O \left[m \left(\frac{\log n}{I} \right)^{\frac{2\alpha}{(2\alpha+1)}} + \frac{\log(n/m)}{m} \right]$$

Multiphoton Microscopy

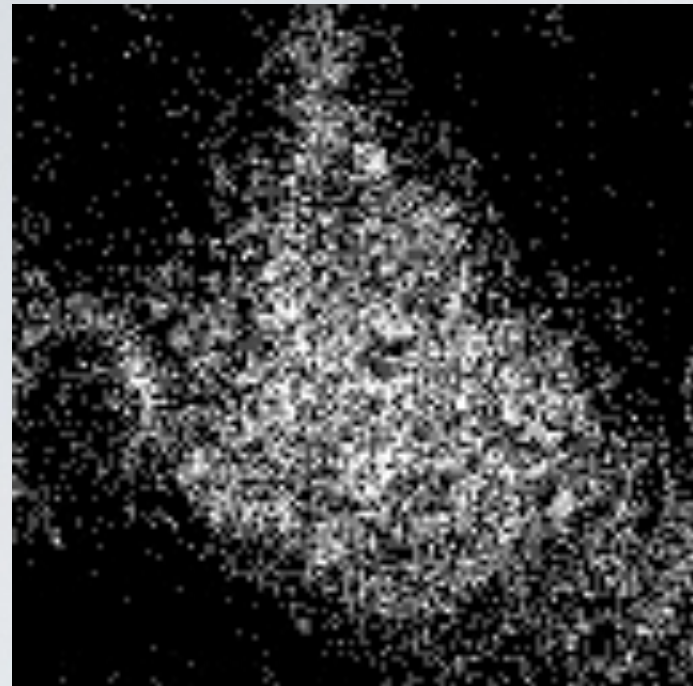
- Data collected for many scan times: what reduction possible?
- Automated regularization tuning via cross-validation
- Use **Poisson thinning** to create two independent images for training and validation
- Cross-validation often preserves theoretical guarantees¹
- Compare against other **fast** denoising methods

SPIRAL-TVX Consistently
Outperforms Other Methods

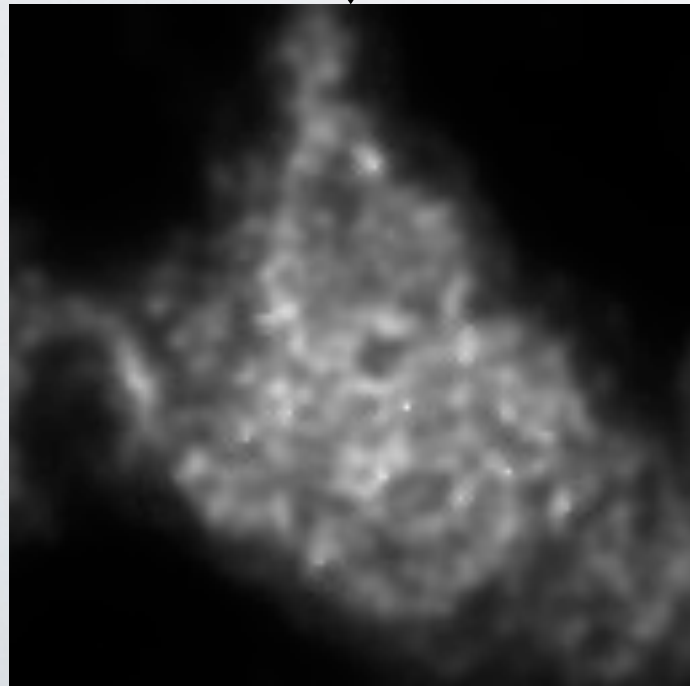
¹Bartlett et al. (2002)

Multi-photon Fluorescence Microscopy

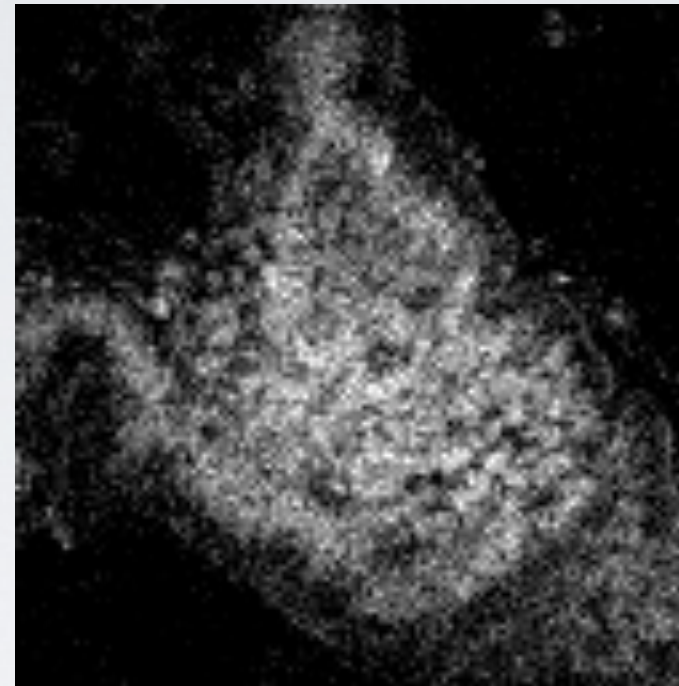
0.1s Scan Time



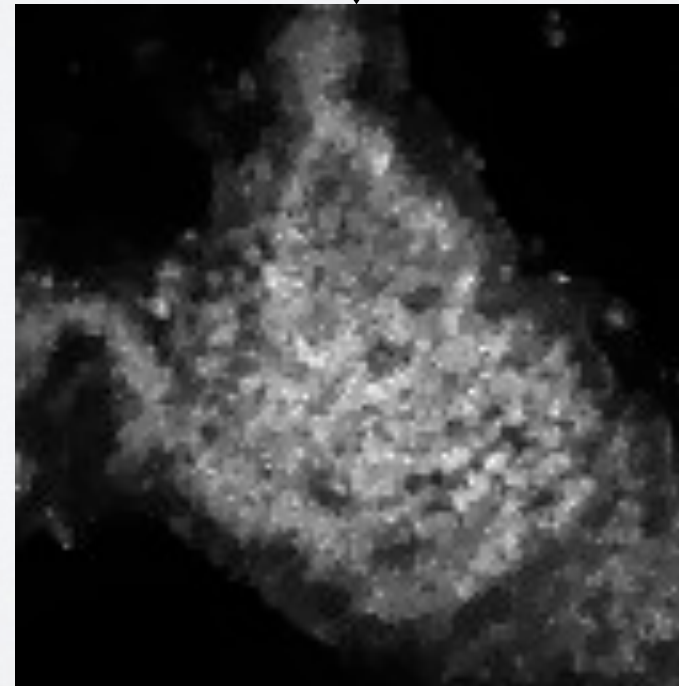
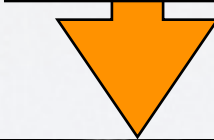
Denoise



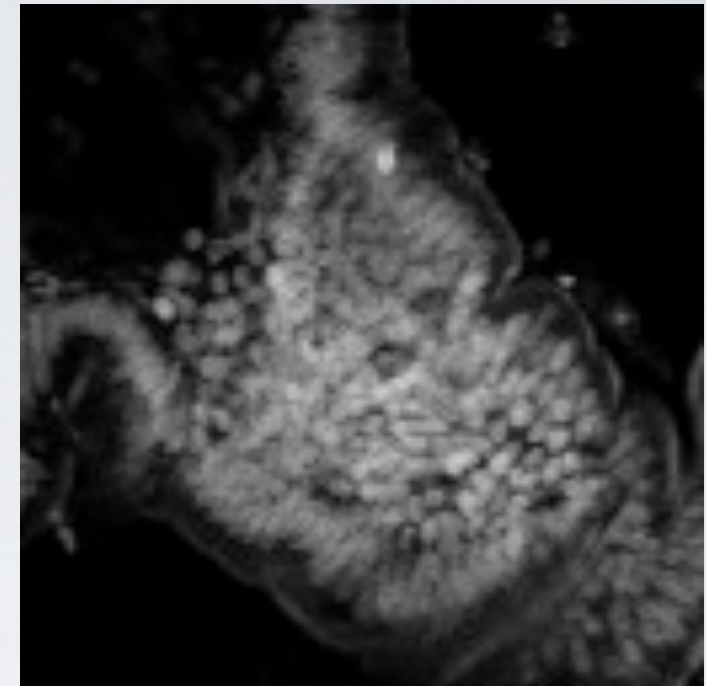
5s Scan Time



Denoise

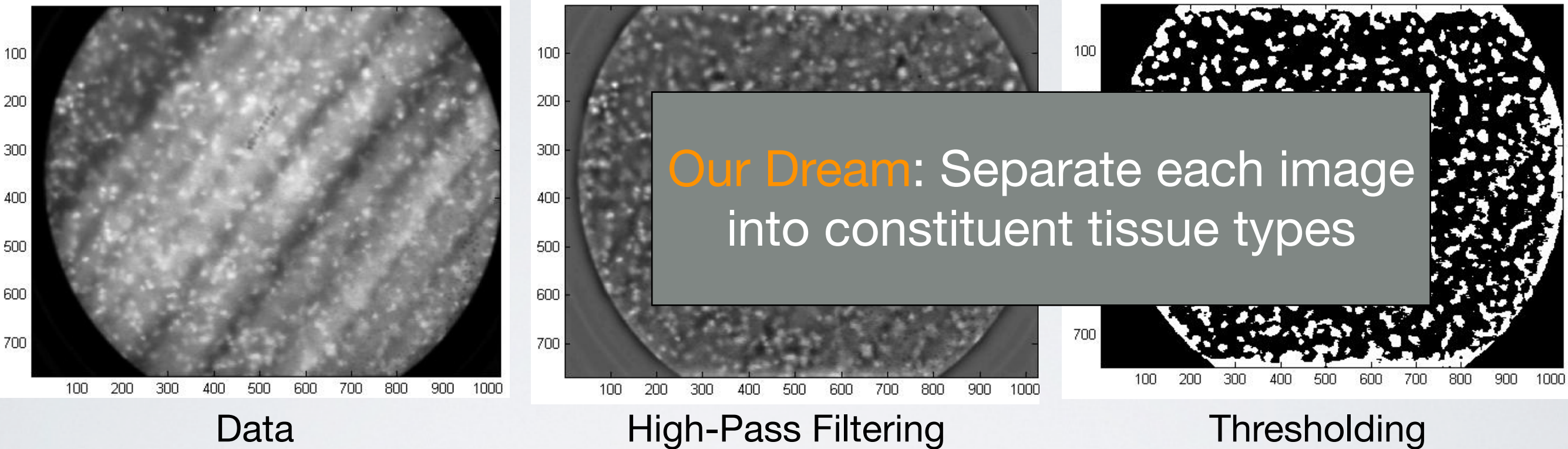


120s Scan Time



Great reduction in
scan times
with similar visual
fidelity

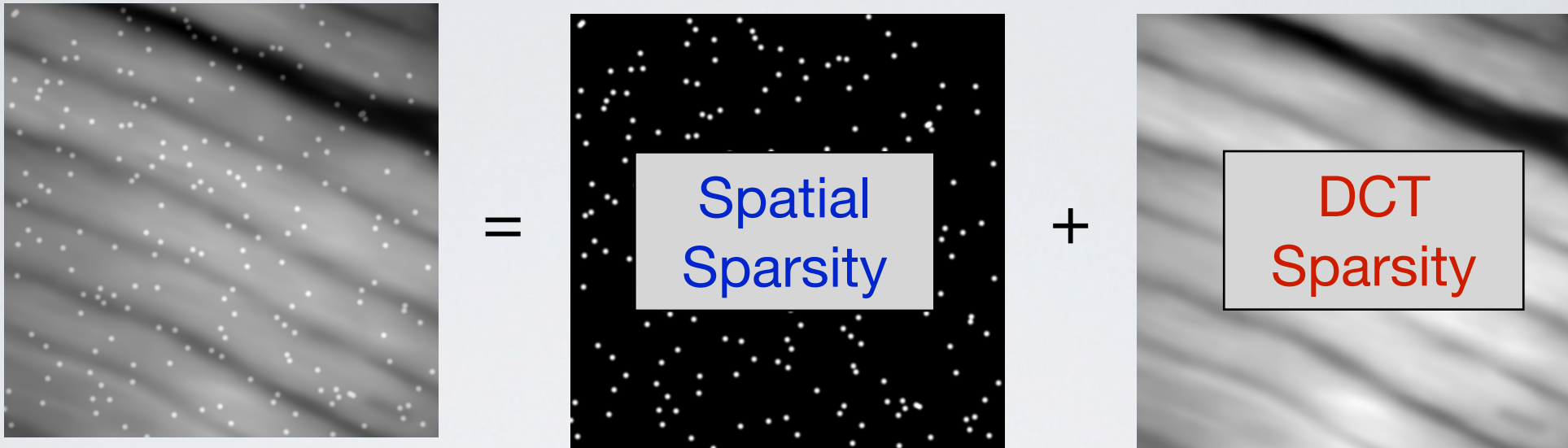
Sparse Decomposition for Margin Assessment



- Only provides estimate of nuclei
- Does not generalize to other tissue types: adipose (fat), fibroglandular tissue (mammography), cross-sectional muscle
- Highly susceptible to photon noise

Challenge: Can we do better?

Sparse Decomposition



True Intensity = Nuclei + Muscle

- Decomposition into components possible if:

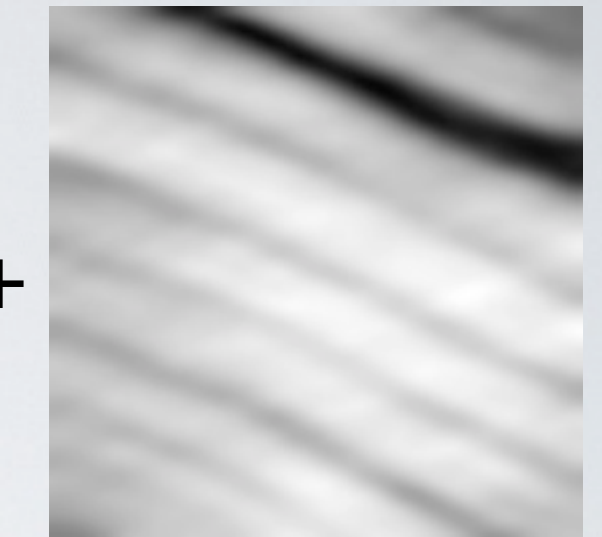
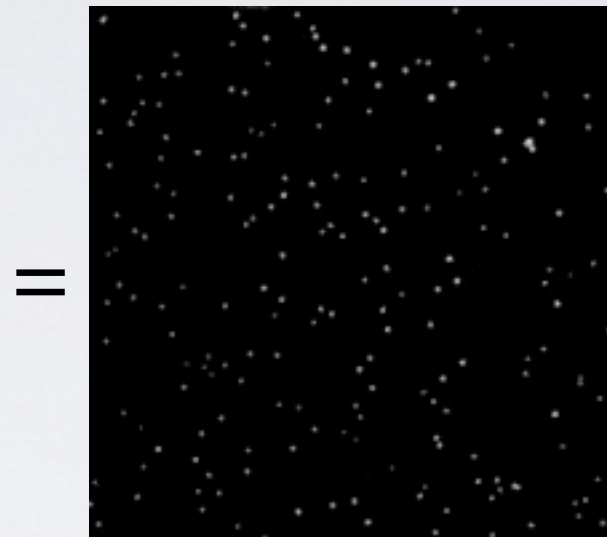
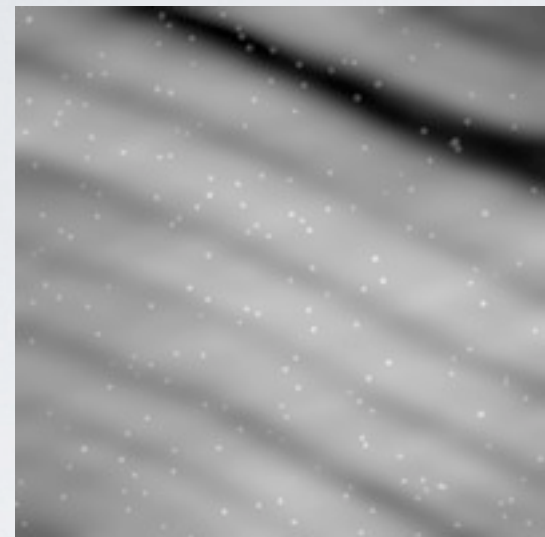
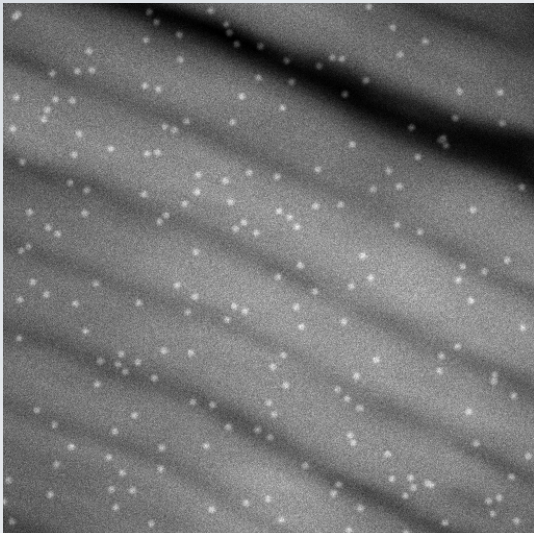
Require each component
to be **sparsely represented**
in mutually **incoherent dictionaries**

$$f = s + F\theta = [I \quad F] \begin{bmatrix} s \\ \theta \end{bmatrix}$$

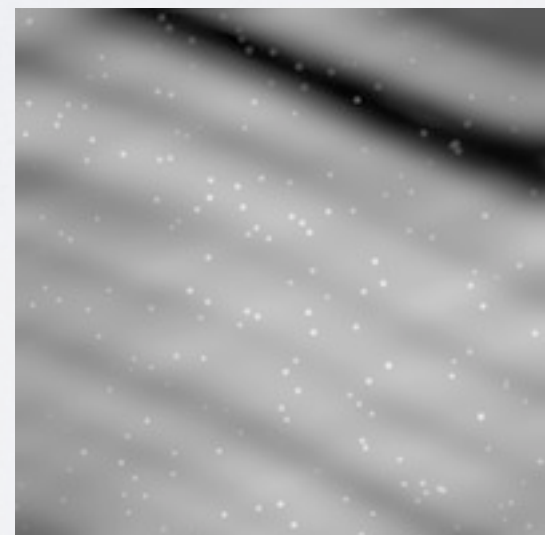
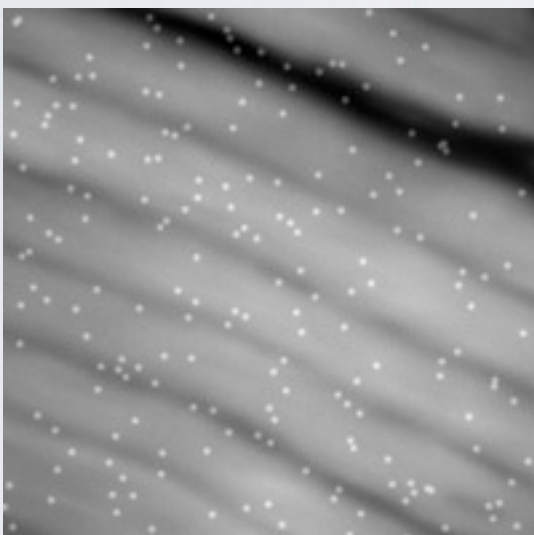
Tight Frame! $W = [I \quad F]$

Simulation Results

Low Intensity:



High Intensity:



Observations

Intensity
Estimate

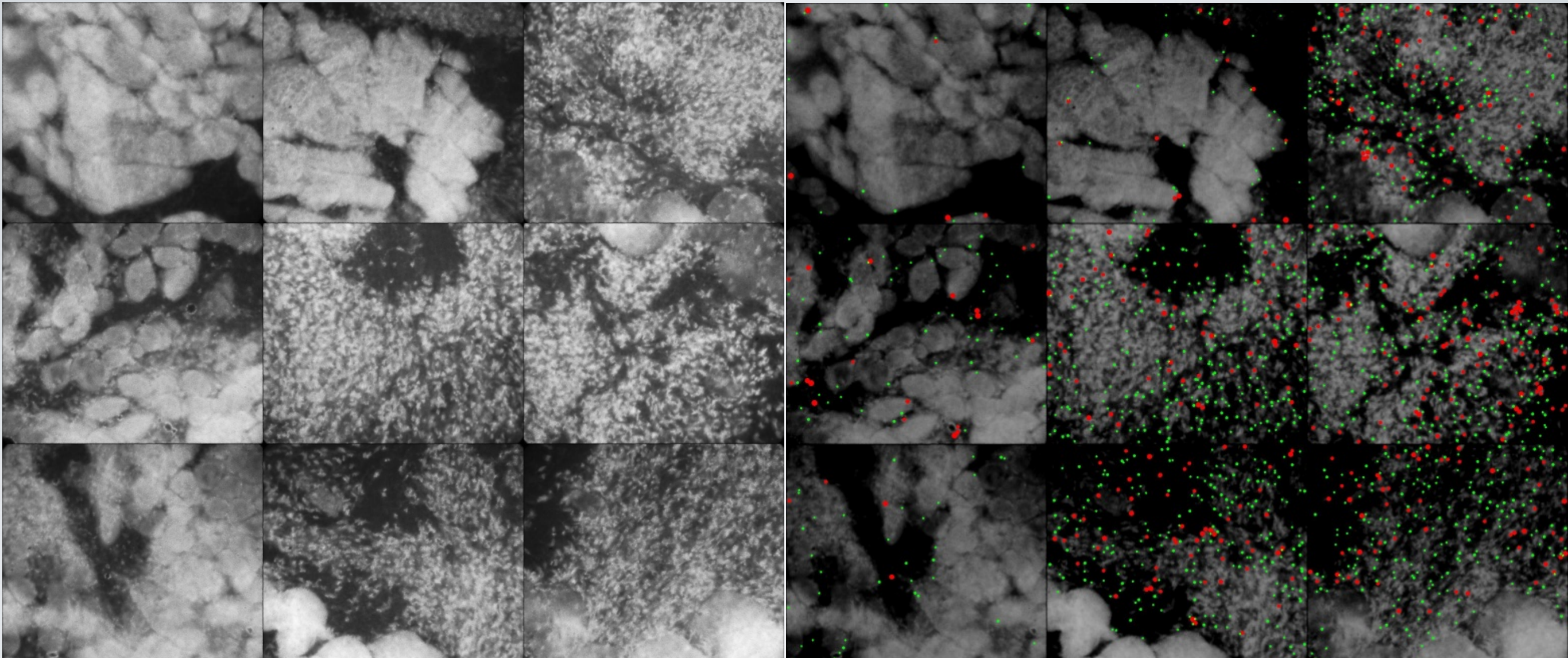
=

Tumor
Estimate

+

Muscle
Estimate

Real Microendoscope Data

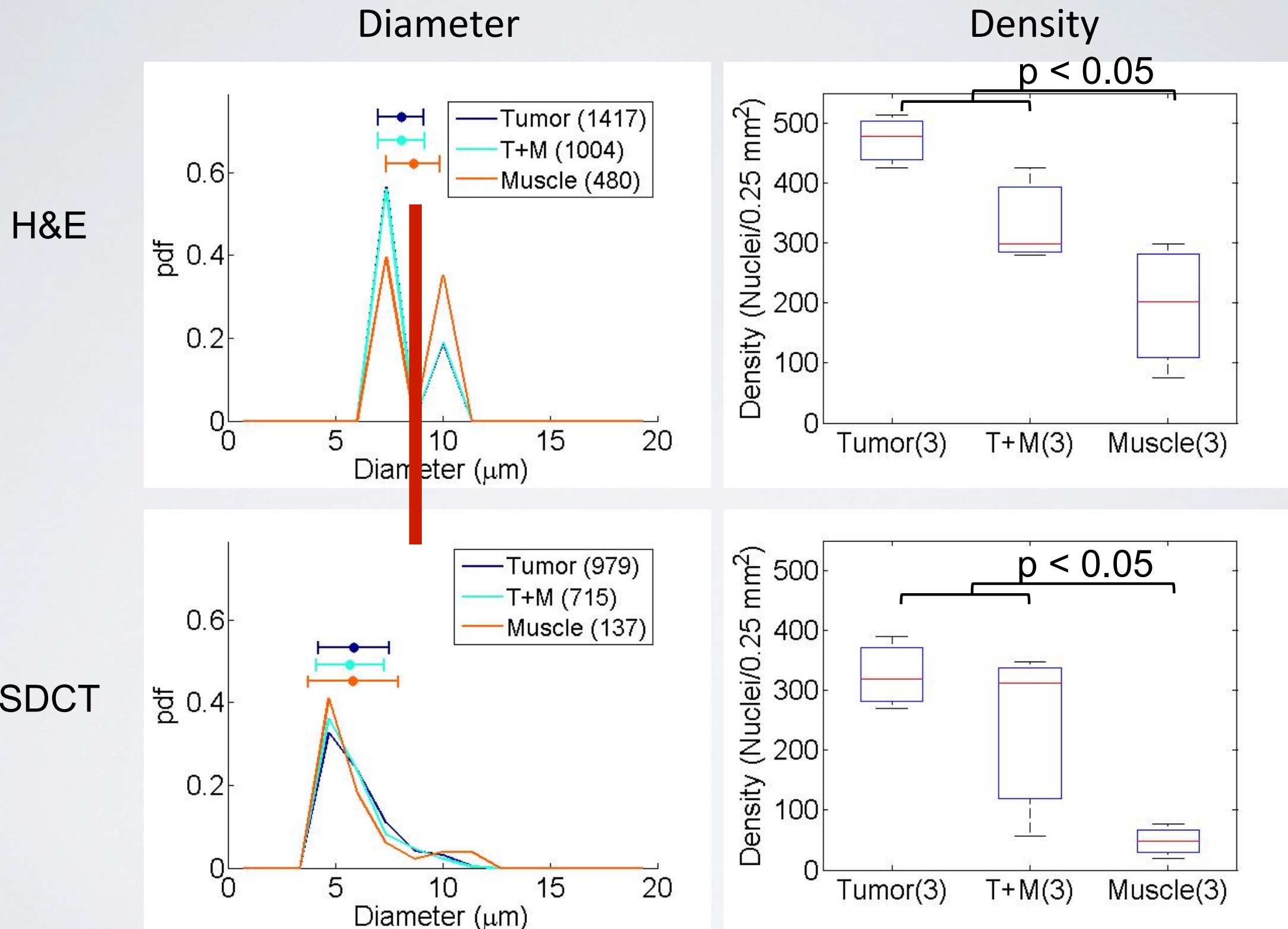


Original Data

Proposed Approach

Red: Larger than 8 μm diameter
Green: Smaller than 8 μm diameter

Size and Density Statistics

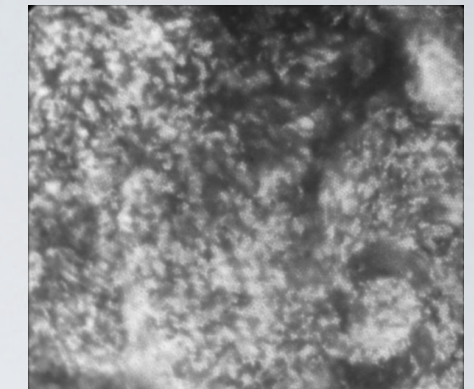


Improve Upon This Method?

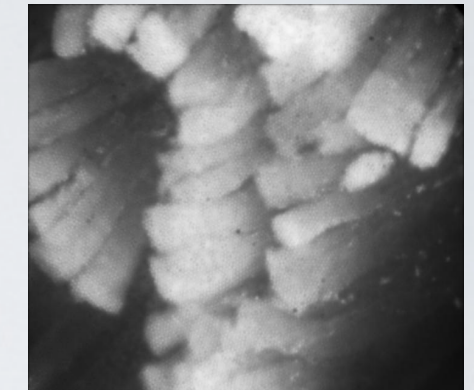
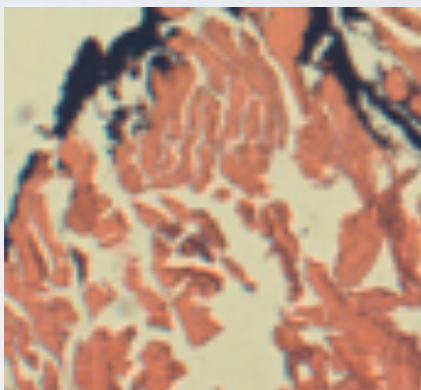
- Biological knowledge:
 - Context for nuclei
- Increase sensing flexibility:
 - Additional contrast agent
 - Spectral characteristics

Given physical constraints
design sensing matrix to
maximize SPIRAL efficiency

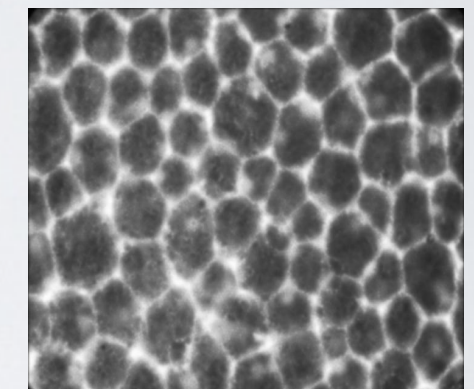
Tumor



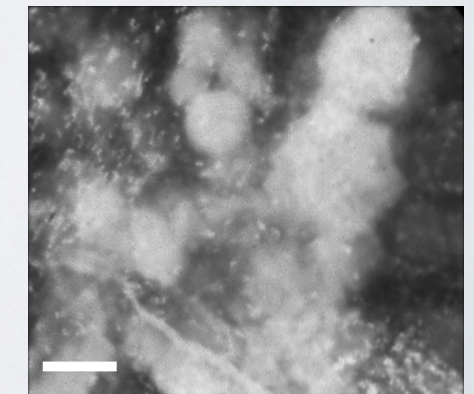
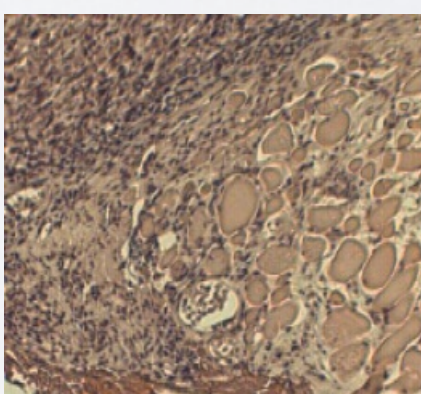
Muscle



Adipose



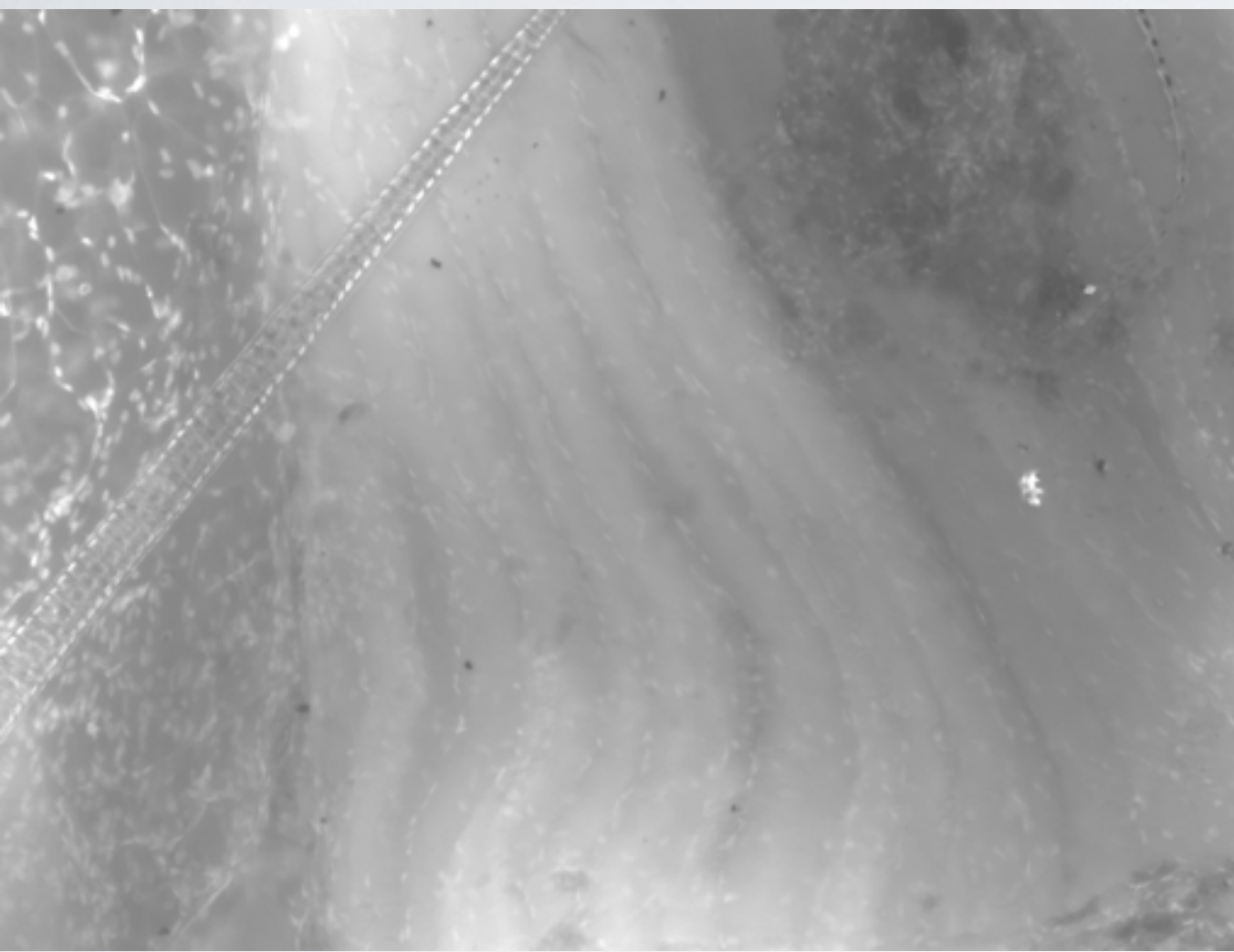
Tumor +
Muscle



Hyperspectral Imaging

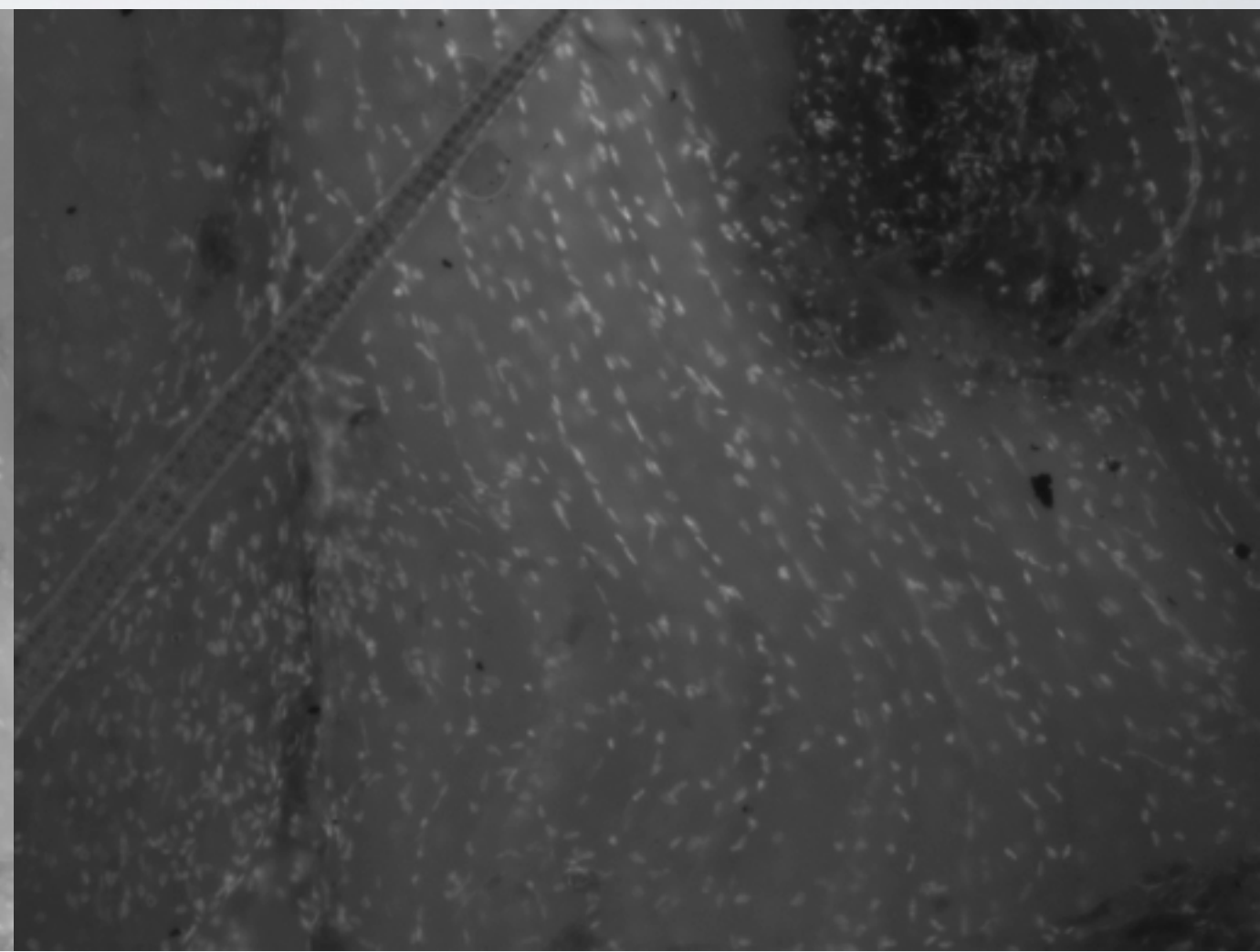
Multiple stains provide information for discriminating tissue
(Different optical filters used for same site)

Proflavine



Approx Equal Uptake

DAPI



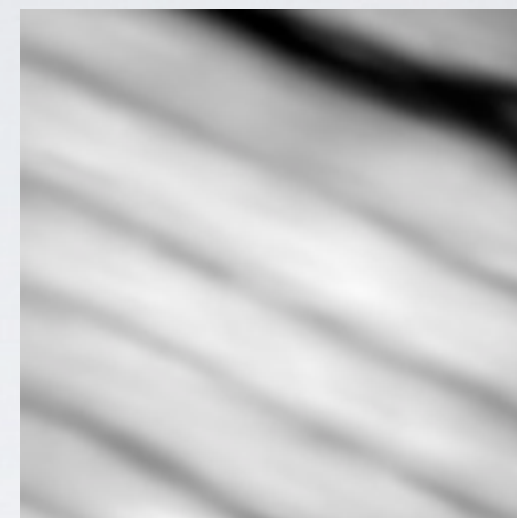
Targets Nuclei

Hyperspectral Imaging

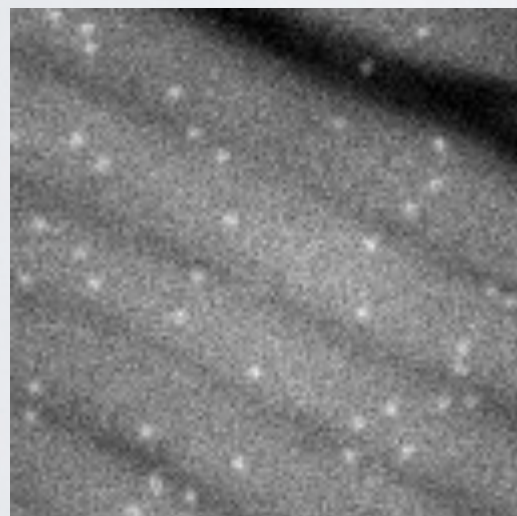
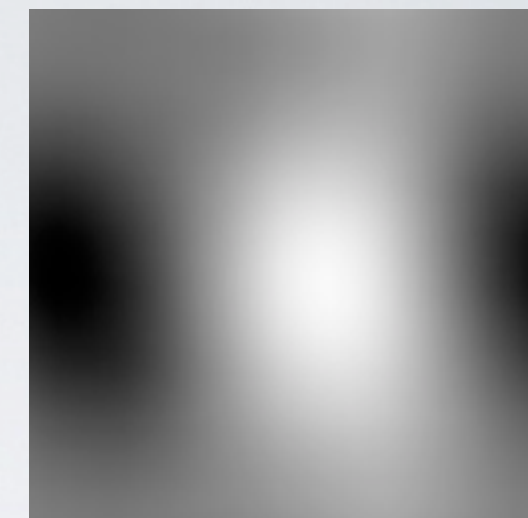
Nuclei



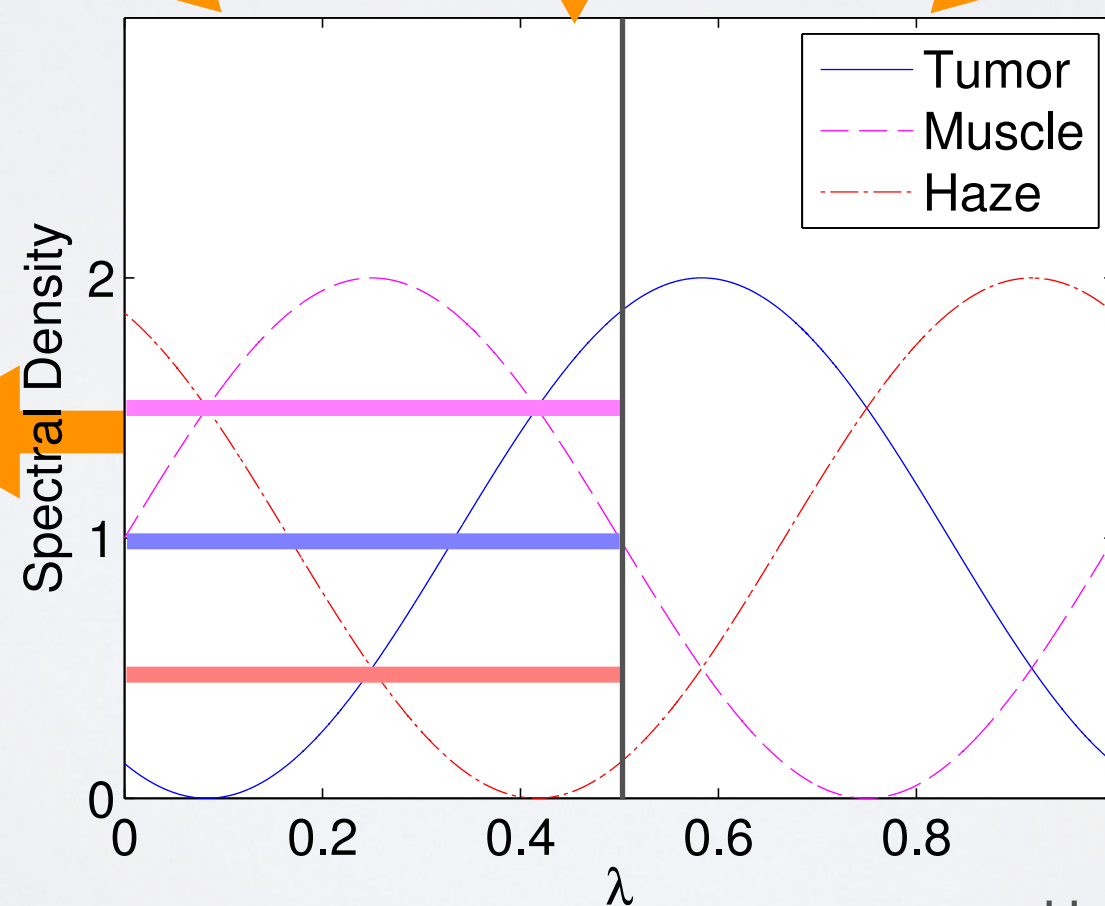
Muscle



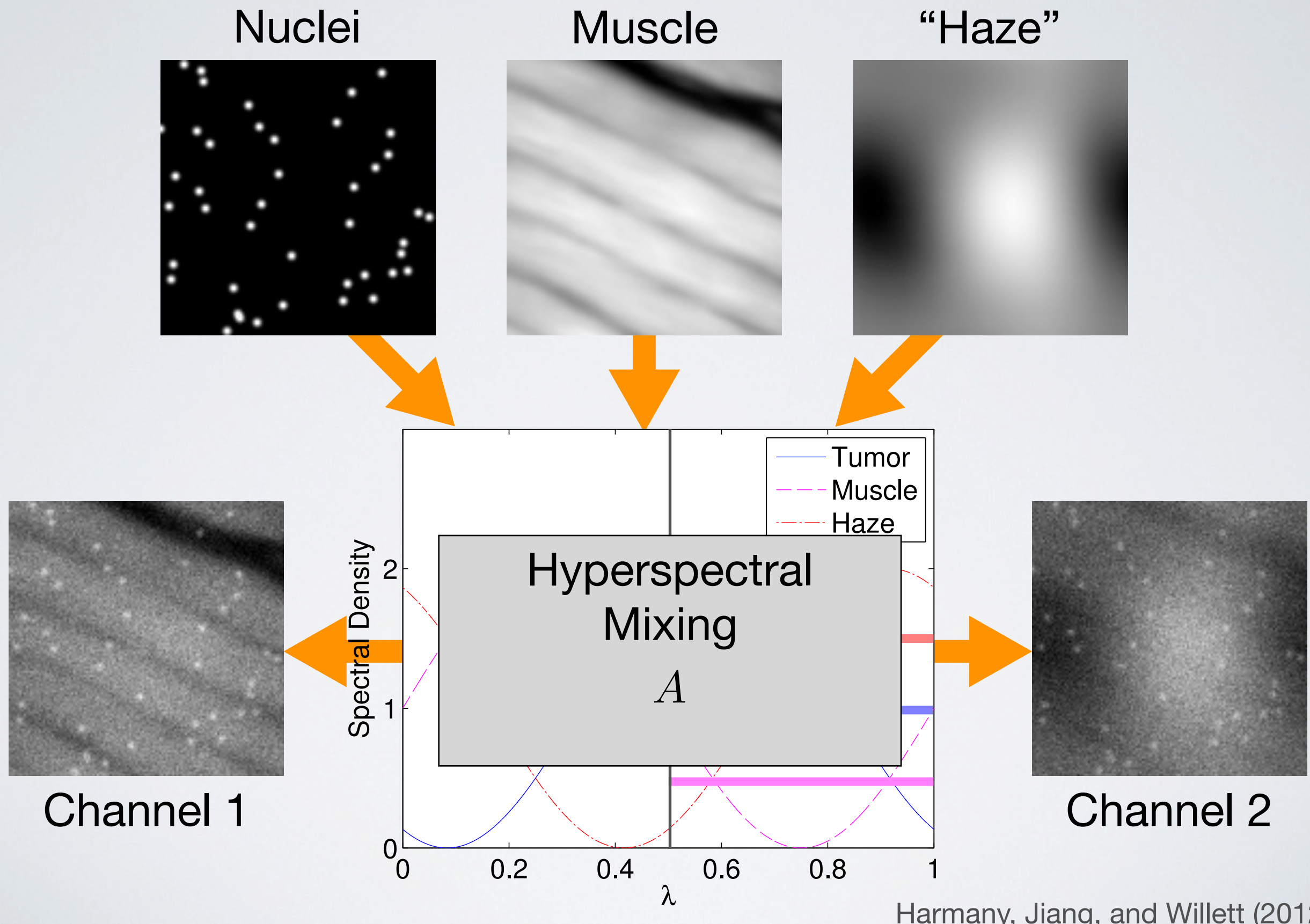
“Haze”



Channel 1

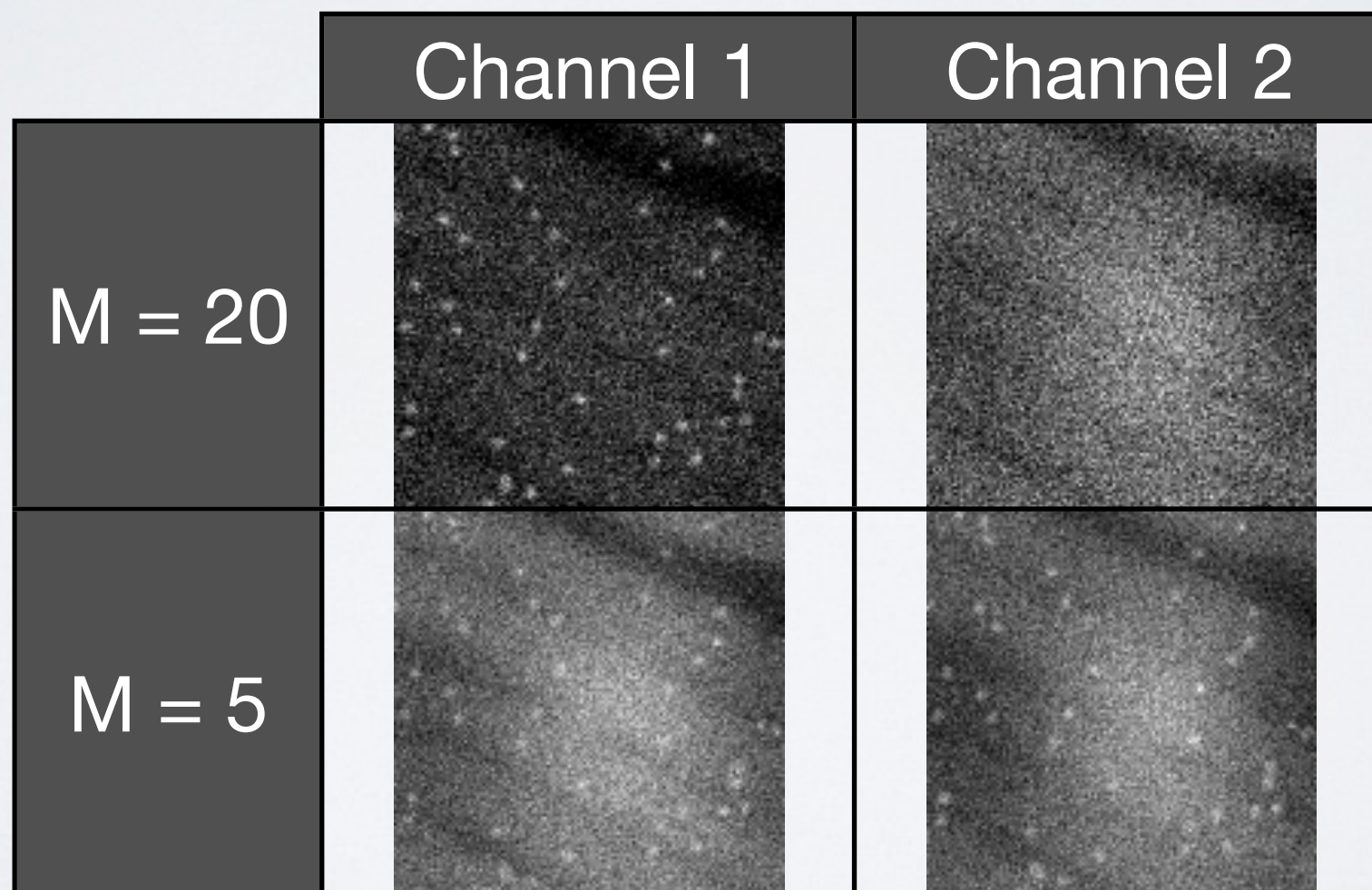


Hyperspectral Imaging

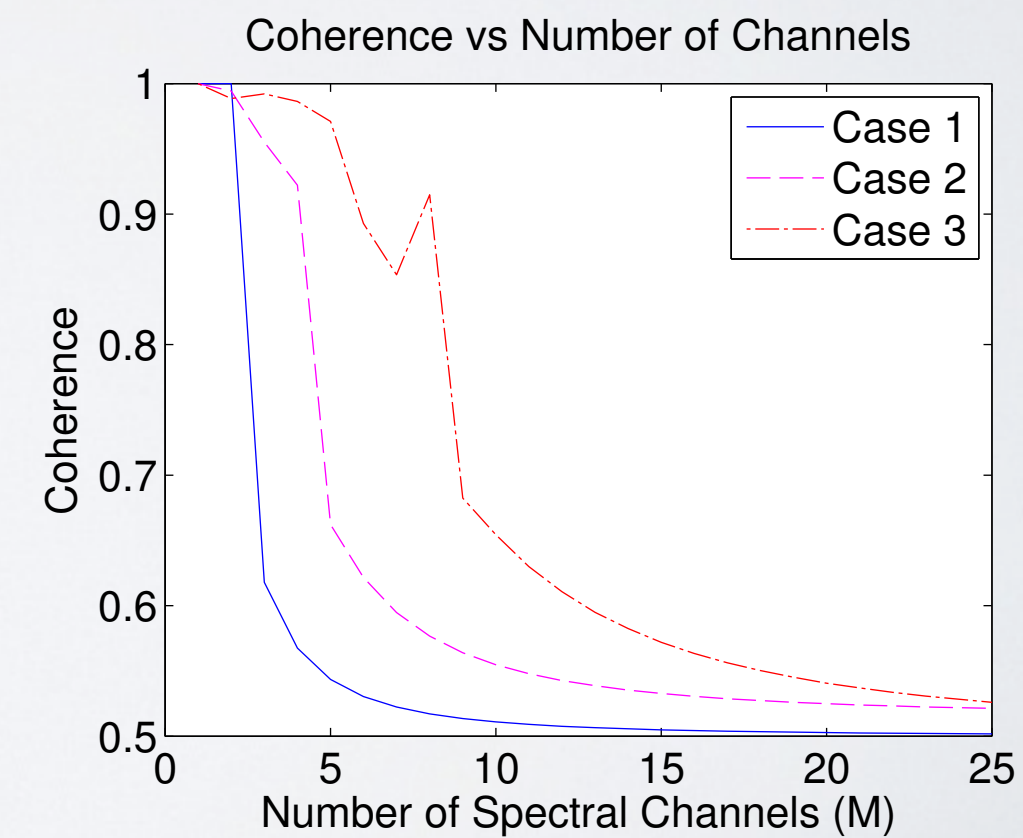
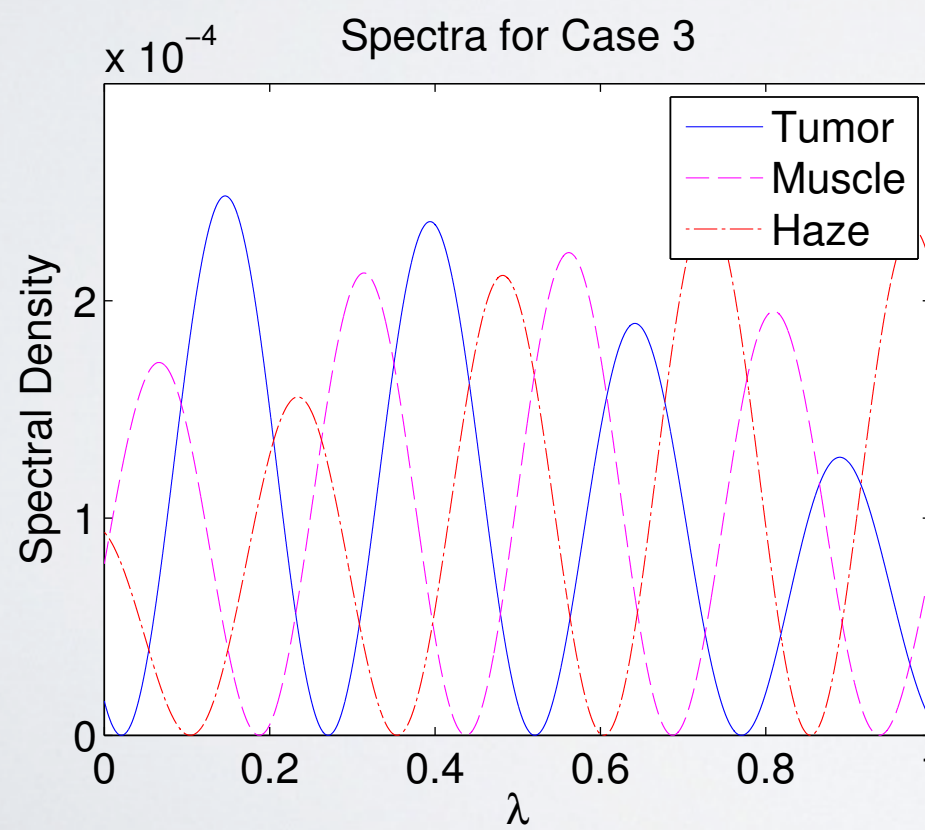
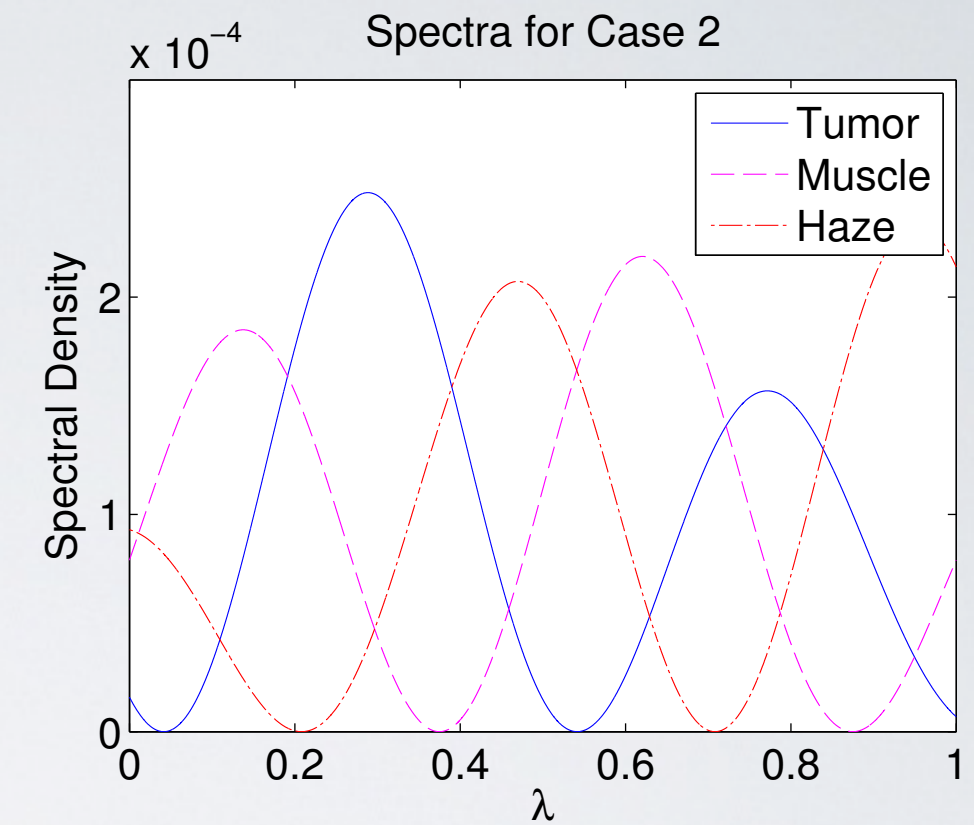
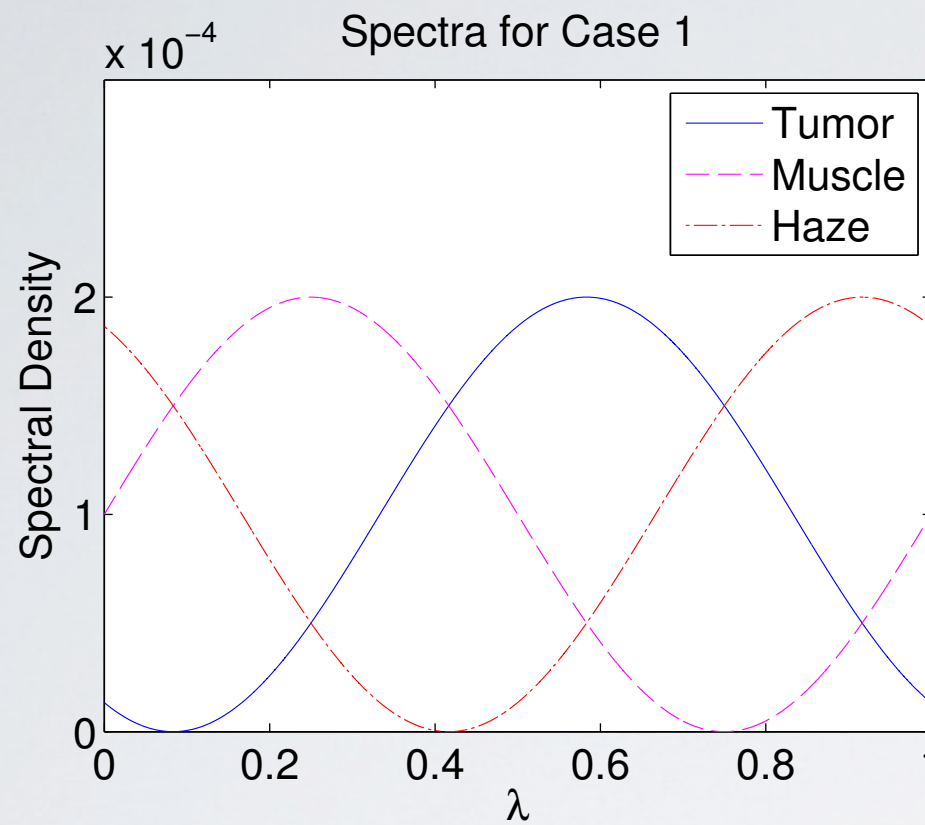


Tradeoffs

- On a fixed intensity budget, need to allocate sensing resources:
 - Too many channels: Low SNR per channel
 - Too few channels: Decreased spectral diversity

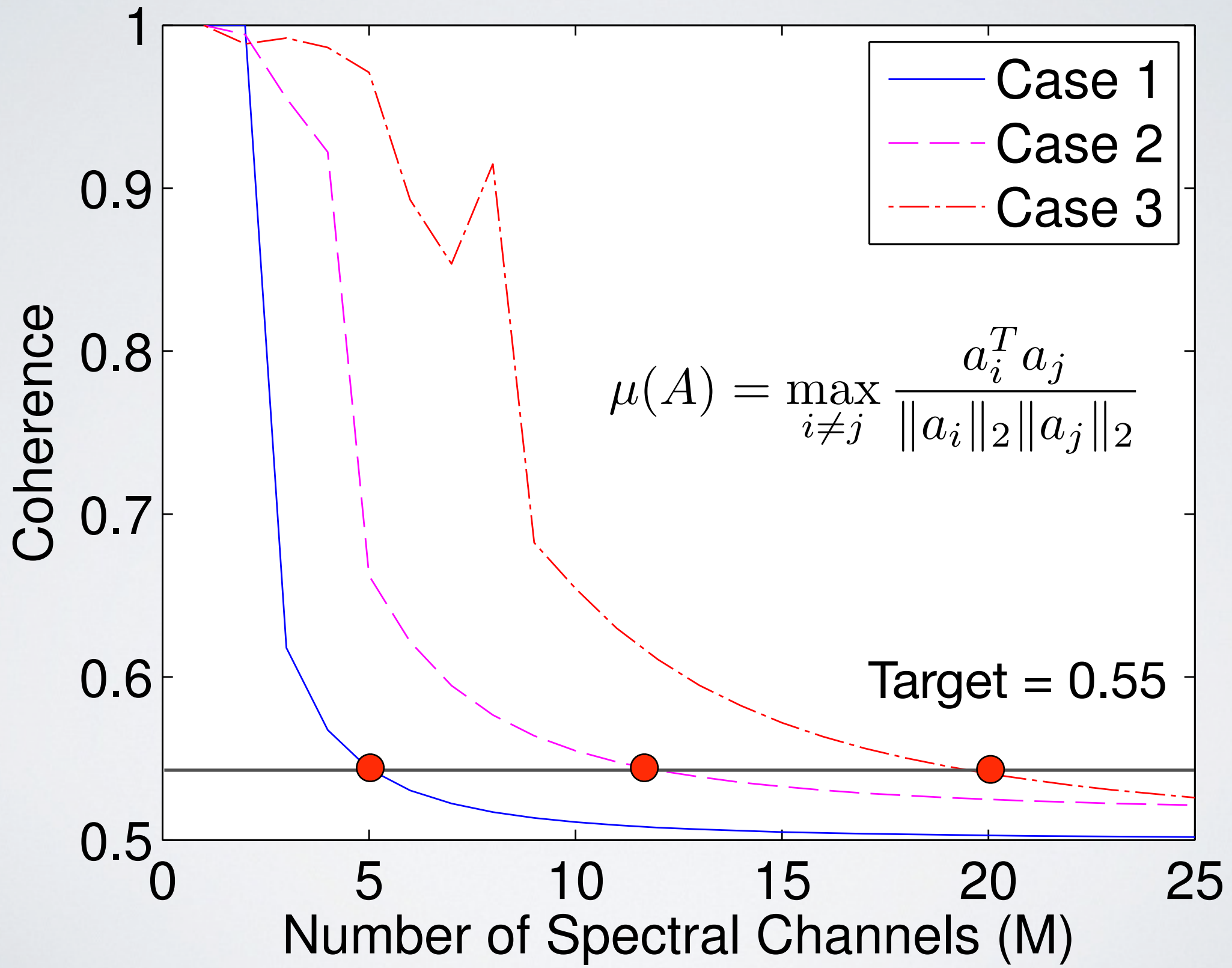


Simulation Results



Simulation Results

Coherence vs Number of Channels

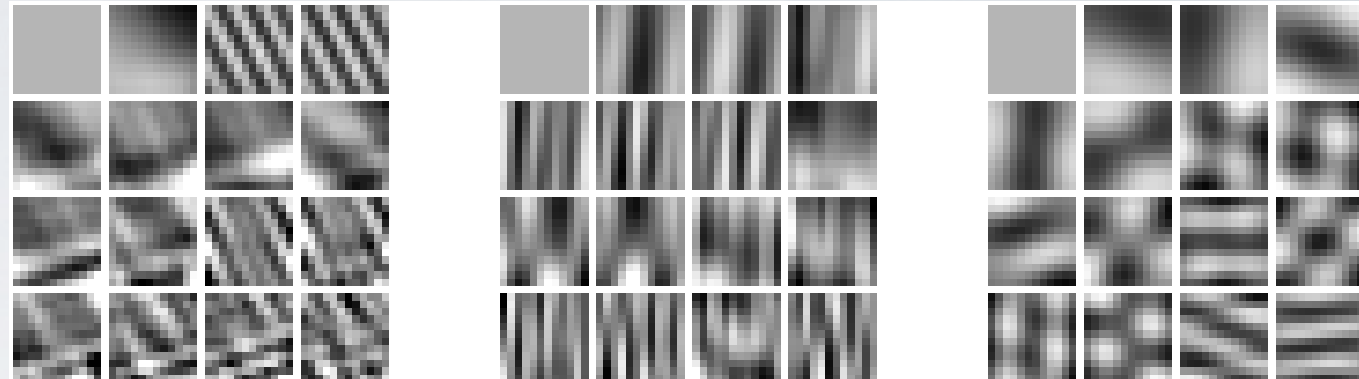


Simulation Results

			Case 1	Case 2	Case 3
$M = 5$	$\mu(A)$	0.5435	0.6621	0.9709	
RMSE (%)	$T/n = 1000$	2.425993	2.578506	5.289591	
	$T/n = 100$	5.938796	6.372602	8.241031	
$M = 12$	$\mu(A)$	0.5077	0.5426	0.6108	
RMSE (%)	$T/n = 1000$	2.392513	2.361507	2.543830	
	$T/n = 100$	5.892149	5.969155	6.295167	
$M = 20$	$\mu(A)$	0.5028	0.5249	0.5407	
RMSE (%)	$T/n = 1000$	2.344829	2.346617	2.330689	
	$T/n = 100$	5.803680	5.769627	5.912512	

Dictionary Learning in Poisson Noise

- Instead of a fixed basis, learn it from data
- Collect training images or **patches** in a matrix: find low-rank approximation
$$F \approx UV$$
- Gaussian data: SVD
- Poisson data: Use SPIRAL for sparse coding¹



Example Dictionary Elements

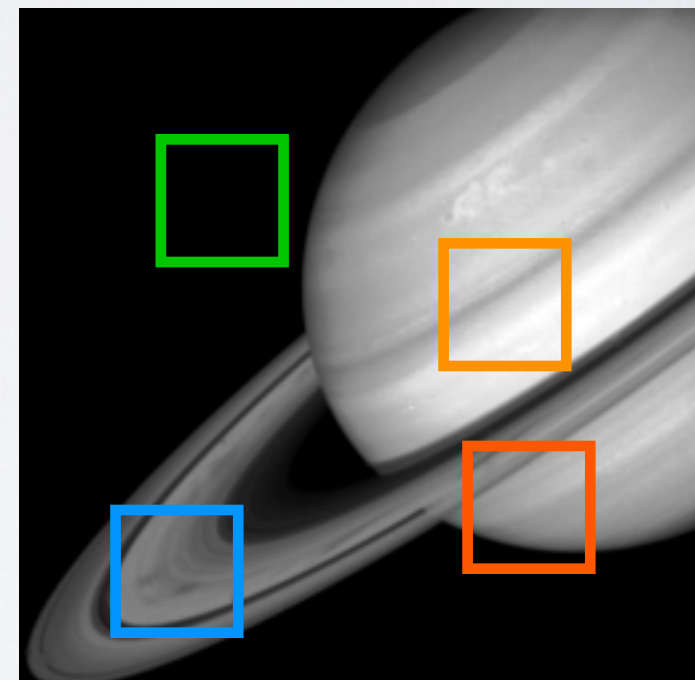


Image Patches

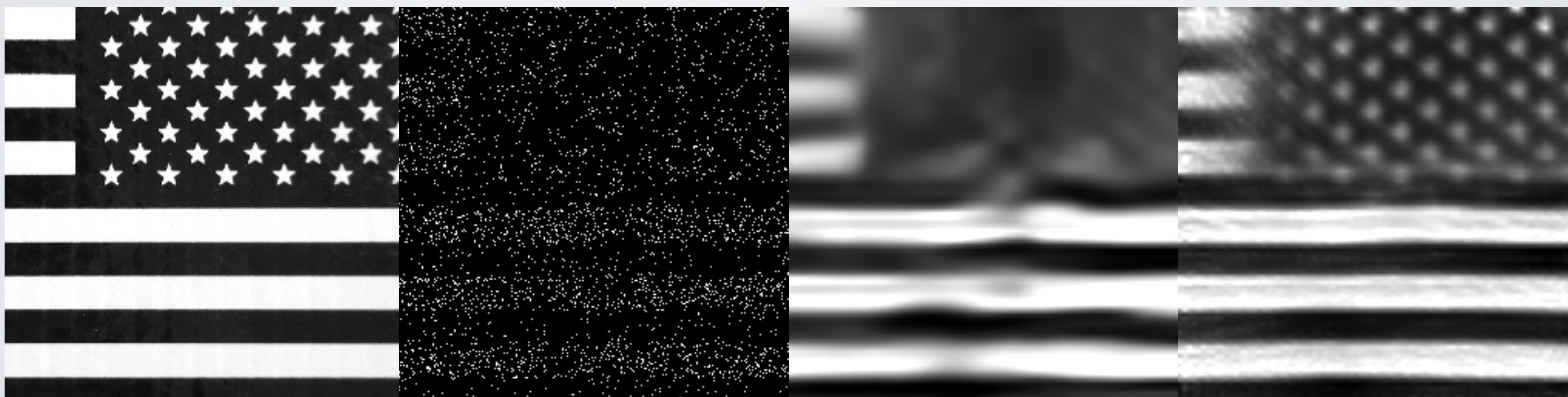
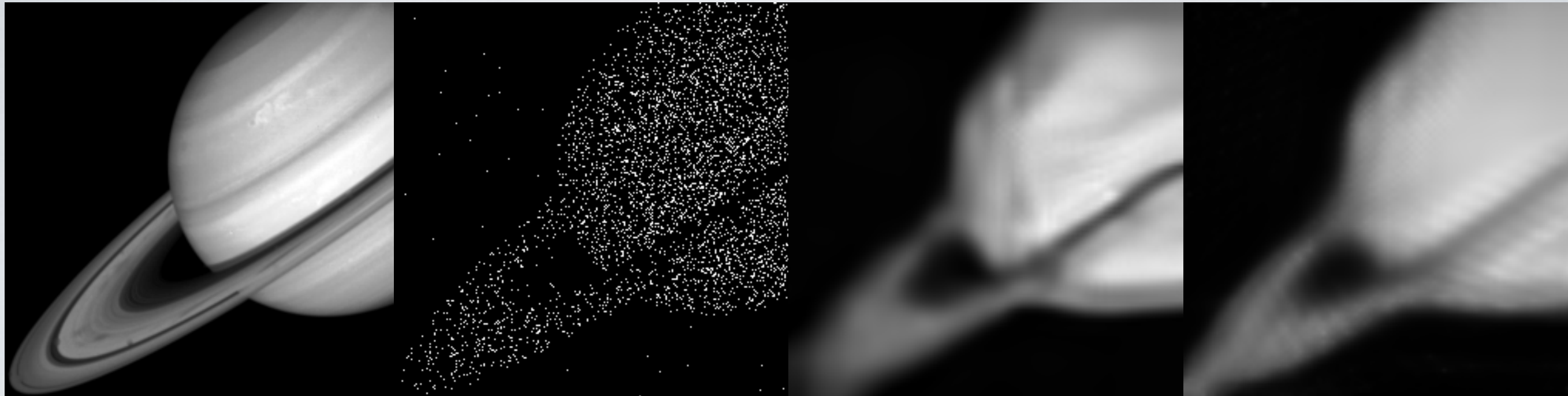
Dictionary Learning in Poisson Noise

Truth

Data

BM3D¹

Proposed²



¹Mäkitalo and Foi (2011); ²Salmon, Harmany, Deledalle, Willett (2012)

Future Directions

- Future applications require **online** algorithms
 - Massive data must be streamed to an algorithm
 - We must update our estimate in a dynamical way
 - Algorithm must make **real-time** decisions
 - Understand tradeoffs when processing data online
- Example: background estimation in video via subspace tracking

Subspace Tracking from Poisson Data

- Other algorithms examined tracking subspaces, but ignore photon limitations (e.g., GROUSE¹, PETRELS²)
- Each frame is a vector in a subspace
Background: Common structure
Foreground: Deviations from subspace
- At each time step we perform two steps:
 - Estimate subspace coefficients (computed via **SPIRAL**)
 - Update the subspace via gradient descent
computationally efficient **rank-1** update
- Online low-rank matrix estimation from Poisson data

¹Balzano et al. (2010), ²Chi et al. (2012)

Subspace Tracking from Poisson Data

Truth



Data

Averaging

Subspace Tracking

Subspace Tracking from Poisson Data

$t = 368$



$t = 1024$



$t = 1400$



Truth

Subspace Tracking

Averaging



Summary of Presented Contributions

- SPIRAL Algorithm
[IEEE Trans. Image Processing 2012, many conference papers]
 - Computationally efficient and widely applicable algorithm
 - Numerical validation on limited-angle SPECT simulation
 - Global convergence guarantees
- Poisson Dictionary Learning
[J. of Mathematical Imaging and Vision 2012, ICIP 2012]
 - State-of-the-art Poisson denoising results
- Tissue Analysis
[Submitted to Radiology, 2012, SSP 2012, SPIE 2011]
 - Promising method for tissue analysis for margin assessment
- Poisson Compressed Sensing
[IEEE Trans. Signal Processing 2010, 2011]
 - Convincingly demonstrated a theoretically predicted effect

Other Contributions

- Coded Aperture Keyed Exposure Sensing
[Submitted to IEEE Trans. Image Processing]
 - Implementable spatio-temporal compressive sensing strategy
 - Performance guarantees based on RIP
 - Numerical validation on SWIR simulation
- Compressive Coded Aperture Imaging
[SPIE 2011, SPIE 2010, SPIE 2009]
 - Method for snapshot compressive imaging
 - Convolution structure yields efficient implementable devices
 - Proposed occlusion detection and optical flow recovery algorithm used to adapt coded aperture mask patterns
- Bounded Signal Recovery
[ICIP 2010, ICASSP 2011 (x2)]
 - Efficient recovery algorithms for signals with known upper and/or lower bounds
 - Demonstrated improved accuracy for signal and video recovery

Thank you!